The Role of SMPD1 in the Innate Immune System's Response to Respiratory Bacterial Infections

Elyse MacFadden-Murphy

Degree of Master of Science

Department of Pharmacology & Therapeutics

Faculty of Medicine

McGill University

Montreal, Quebec, Canada

January 30th 2015

A thesis submitted to McGill University in partial fulfillment of the requirements of the degree of Master of Science

©Copyright 2015 All rights reserved.

ACKNOWLEDGMENTS

There are many people whom I would like to thank for helping me complete my Masters' Thesis over the past two years. It has been a great experience and I have learned a tremendous amount not only about science, but also myself.

First and foremost, I wish to thank my supervisor Dr. Simon Rousseau who gave me the opportunity to carry out my project in his lab. His guidance and support helped me succeed and I am truly grateful to have been one of his students. I would also like to thank the Department of Pharmacology & Therapeutics, in particular my committee members, Dr. Stephane Laporte, Dr. Barbara Hales and Dr. Guillmera Almazan, for all their help along the way.

To Julie, Guy, Lucie, and Mirai thank you for helping me daily throughout my time at the lab. I cannot thank you enough for all your time and efforts in helping me learn and develop my project. Of course Trevor, and Raquel I would like to thank you for your support and friendship; it was very much appreciated over the past two years. It was a pleasure working with all of you.

Finally, I wish to thank my family and friends, especially my parents and Jason. Without all of your help and encouragement I would not be where I am today. You have all helped me to achieve my goals, and I thank each and everyone one of you.

TABLE OF CONTENTS

ACKNOWLEDGMENTS	ii
TABLE OF CONTENTS	iii
LIST OF TABLES	V
LIST OF FIGURES	
CHAPTER 1: INTRODUCTION	3
1.1. Pertinent Respiratory Diseases	3
1.1.1. Niemann-Pick Disease and SMPD1:	3
1.1.2. Cystic Fibrosis:	7
1.2. Cell Signalling	9
1.2.1. Mitogen Activated Protein Kinases:	9
1.2.2. Airway Epithelial Cells:	. 12
1.2.3. Innate Immune Response Through TLR Signalling:	. 14
1.2.4. NFĸB Signalling:	. 16
1.2.5. Ceramide/Sphingolipid Pathway:	. 18
1.3. Signalling Involved with SMPD1 in Context of Innate Immunity	. 21
1.3.1. p38α:	
1.3.2. Cytokine Production:	. 23
1.4. Rational and Objectives	. 24
CHAPTER 2: Materials and Methods	. 26
2.1. Materials	. 26
2.1.1. Preparation of <i>P. aeruginosa</i> diffusible material	. 26
2.2. Methods	. 27
2.2.1. Cell Culture	. 27
2.2.2. Construction of Flp-IN cells	. 27
2.2.3. Creation of stable BEAS-2B with shRNA to SMPD	. 29
2.2.4. Cell Lysis and Immunoblot	. 30
2.2.5. Cell Survival	. 32
2.2.6. ELISA (Enzyme Linked Immunosorbent Assay)	
2.2.7. SMPD1 Enzyme Activity Assay	. 32
2.2.8. FRET	. 33
2.2.9. Immunofluorescence	. 33
2.2.10. Tandem Affinity Purification (TAP)	. 34
2.2.11. Mass Spectrometry	. 36
2.2.12. NFkB Reporter Assay	. 37
2.2.13. Neutrophil Migration Assay	. 37
2.2.14. RNA Isolation and cDNA Synthesis	. 38
2.2.15. Quantitative PCR	. 39
2.2.16. Statistical Analysis	. 40
CHAPTER 3: Inhibition of SMPD1 Disrupts MAPKs and NF κ B Signalli	ng
Pathways	. 41
3.1. Rationale	. 41
3.2. The impact of pharmacological inhibition of SMPD1 is ambiguous concerning the	าе
phosphorylation of p38 $lpha$	
3.3. RNA interference of SMPD1 to investigate its role in p38 α MAPK phosphorylation	ion43
3.3.1. Developing a doxycycline-inducible short hairpin RNA to decrease SMP	D1
in airway epithelial cells	. 43
3.3.2. AECs with SMPD1 knocked-down have dysregulated MAPKs activation	46

3.3.3. p38 α MAPK activation can be rescued in sh-SMPD1 cells when transc	
with wild-type SMPD1	
3.4. NFκB Activation is lowered in AECs when transfected with an inactive form of	f
SMPD1	50
3.5. Elevated levels of reactive oxygen species (ROS) in sh-SMPD1 AECs	51
3.6. Conclusion	53
CHAPTER 4: SMPD1's Role in the Proper Functioning of the Innate	
Immune System Involves Cytokine Regulation and Consequently Neutro	phil
Recruitment	-
4.1. Rationale	56
4.2. Airway epithelial cells lacking SMPD1 exhibit hyper-secretion and increased	
expression levels of cytokines	57
4.2.1 Higher concentrations of IL-6 and IL-8 are secreted from AECs with	
SMPD1 knocked-down when challenged with PsaDM	57
4.2.2 An overall increase in cytokine expression exists in sh-SMPD1 AECs	
4.2.3. Caspase-1 dependent cytokines also elevated in sh-SMPD1 AECs	
4.3. A consequence of elevated cytokine levels in sh-SMPD1 AECs is the recruitn	
of more neutrophils	
4.4 Conclusion	
CHAPTER 5: Disruption of Intracellular Localization and Protein-Protein	า
Interactions of the SMPD1 (L225P)-disease causing-mutant	
5.1. Rationale	66
5.2 SMPD1 (L225P)-disease causing-mutant shows impaired translocation to out	
leaflet of cell membrane by immunofluorescence	
5.3.Identification of potential novel binding partners of SMPD1 using tandem affini	
purification followed by mass spectrometry analysis	-
5.4. Conclusions	
Chapter 6: Conclusions and Future Directions	74
6.1. Summary of Results and General Discussion	
6.1.1. SMPD1 is required for the appropriate activation of MAPKs in AECs to	
trigger the necessary immune response when faced with bacterial challenge	
6.1.2. AECs lacking SMPD1 demonstrated an over-production of various	
cytokines implicated in inflammation and significantly more neutrophils recru	ited75
6.1.3. Impaired translocation of SMPD1 (L225P)-disease causing-mutant to	
outer-leaflet of the cell membrane upon bacterial stimulation	
6.1.4. Potential novel protein interactions of SMPD1	
6.2. Conclusions	
6.3. Future Directions	
References	
Appendix	

LIST OF TABLES

Table 1: Primers for Flp-In System	29
Table 2: Primers for shRNA Knockdown	29
Table 3: Antibodies For Immunoblots	31
Table 4: Primers for qPCR	40
Table 5: Brief Description Cytokines Analyzed	60
Table 6: Top hits identified from mass spectrometry analysis using	
PANTHER Classification System 9.0.	73

LIST OF FIGURES

Figure 1: Translocation of SMPD1 from Lysosome to Outer-leaflet of	
Membrane to Produce Ceramide (Adapted ⁷)	4
Figure 2: Graphical Representation of Potential Glycosylation Sites	
(adapted ¹⁵)	5
Figure 3: Simplistic View of the Cascade of Sequential	
Phosphorylations in MAPK Pathway	
Figure 4: Activation of MAPK Signalling Pathway ⁵⁷	
Figure 5: Pseudostratified Airway Epithelium ^{59,62}	13
Figure 6: Normal innate immune system's defence against bacterial	
infection involves activation of p38 α MAPK through TLRs (adapted from 6	^{;8})
Figure 7: Canonical NFκB Signalling Pathway (adapted from ⁷³)	
Figure 8: Sphingomyelin/Ceramide Pathway	
Figure 9: TAP Tag in HEK-Flp-In Cells	29
Figure 10: Phosphorylation of p38 α MAPK in the presence of SMPD1	
inhibitors.	
Figure 11: Creation of stable Beas-2B AECs with sh-RNA against SMPD	
Figure 12: Phosphorylation of p38 α MAPK in stable Beas-2B AECs with ϵ	
RNA against SMPD1.	
Figure 13: Phosphorylation of ERK1/ERK2 MAPK in stable Beas-2B AEC	
with sh-RNA against SMPD1.	
Figure 14: Phosphorylation of JNK MAPK in stable Beas-2B AECs with s	
RNA against SMPD1.	48
Figure 15: Rescue experiment of the phosphorylation of p38 α MAPK in	
stable Beas-2B AECs with sh-RNA against SMPD1	
Figure 16: Measurement of NF κ B activity in Beas-2B AECs reporter cells	
with WT and L225P mutant SMPD1 transferred	
Figure 17: FRET analysis of stable Beas-2B AECs SMPD1-shRNA cell in	
the presence of H ₂ O ₂ .	
Figure 18: Cell survival in the presence of H ₂ O ₂ as an inducer of reactive	
oxygen species.	
Figure 19: Measurement of secreted IL-6 and IL-8 by ELISA in stable Be	
2B AECs SMPD1-shRNA cells.	58
Figure 20: Time course of mRNA expression levels of various cytokines	
upon 3 hr PsaDM stimulation in stable Beas-2B AECs SMPD1-shRNA ce	
Figure 04. Francisco levelo of access 4 december and bits.	
Figure 21: Expression levels of caspase-1 dependent cytokines	
Figure 22: Neutrophil recruitment assay.	64
Figure 23: Immunofluorescence in Hek-Flp-IN cells expressing WT or	00
L225P mutant SMPD1.	
Figure 24: TAP SDS-PAGE gel.	
Figure 26: Venn diagrams of preliminary analysis o d mass spectrometry	
data using Scaffold Viewer program	93

ABBREVIATIONS and SYMBOL

Three-nucleotide deletion at the 508th codon in

 Δ F508 CFTR causing the deletion of a phenylalanine residue

 $\begin{array}{ccc} \mu L & & \text{Microliter} \\ \mu m & & \text{Micrometer} \\ \mu M & & \text{Micromolar} \\ \text{ACN} & & \text{Acetonitrile} \end{array}$

AEC Airway Epithelial Cells

Ami Amitriptyline

ANOVA Analysis of Variance

ASK1 Apoptosis signal-regulating kinase 1

ASMKO Acid Sphingomyelinase Knockout
ATCC American Type Culture Collection

ATP Adenosine tri-phosphate

BEAS-2B Immortalized human bronchial epithelial cells

BIRB0796 p38 MAPK inhibitor

BSA Bovine Serum Albumin

CaCl₂ Calcium Chloride

CARD Caspase recruitment domain

cDNA Complimentary deoxyribonucleic acid

CF Cystic Fibrosis

CFTR Cystic Fibrosis transmembrane conductance regulator

cm Centimetres

CM Conditioned media

CnT17 Airway epithelium Medium, Cell-n-Tec

CO₂ Carbon dioxide

CSF colony-stimulating factors

DMEM Dulbeccos Modified Essential Medium

Dnase DNA cutting enzyme

Dox Doxycycline

dsDNA Double stranded Deoxyribonucleic acid

dsRNA Double stranded ribonucleic acid

DTT Dithiothreitol

EDTA Ethylenediaminetetraacetic acid
EGTA Ethylene glycol tetraacetic acid

ELISA Enzyme linked immunosorbtion assay

ERK Extracellular signal-regulated protein kinases

FBS Fetal bovine serum

GM-CSF Granulocyte Macrophage Colony Stimulating Factor

H₂O₂ Hydrogen Peroxide

HCI Hydrochloric acid

HeLa Helen Larson cells (human uterine cervical carcinoma cells)

HPLC High pressure liquid chromatography

hr Hour

HSP33 Redox regulated molecular chaperone

IgG Immunoglbulin G

IKK IkB Kinase
IL Interleukin

IL-R Interleukin Receptor

IRAK IL-1R-associated kinase

JNK c-Jun N-terminal kinase

L225P Mutant SMPD1
LPS Lipopolysacchride

M Molar

MAP2K of MKK MAPK kinases

MAP3K MAPK Kinase Kinases

MAPK Mitogen activated protein kinase

MAPKAP Mitogen activated protein kinase

MAPKAPK2 MAPK activated protein kinase-2

M-CSF Macrophage Colony Stimulating Factor

MDA5 Melanoma differentiation associate protein 5

MEKK3 MAPK/ERK kinase kinase 3

MgCl₂ Magnesium Chloride

min Minutes
mL Millilitre
mm Millimetre
mM Millimolar

mRNA Messenger ribonucleic acid

MS Mass Spectrometry

MSK Mitogen and stress activated kinases

Myd88 Myeloid differentiation primary-response protein

nm Nanometer

nM Nanomolar

NO Nitrogen Oxide

°C Degrees Celsius
OD Optical Density

P/S 100U penicillin G and 100 ug/mL streptomycin

PA Pseudomonas aeruginosa

PAMPs Pathogen Associated Molecular Patterns

PAO1 Laboratory strain of *Pseudomonas aeruginosa*

PBS Phosphate buffered saline

pH Presence of Hydrogen

PRR Pathogen Recognition Receptors

PsaDM P. aeruginosa diffusible material

qPCR Quantitative real time polymerase chain reaction

RANTES Regulated on Activation, Normal T-cell Expressed and Secreted

rcf Relative centrifugal force

RLU Relative luciferase units

s Seconds

S1P Sphingosine-1-Phosphate

SD Standard deviation

SDS-PAGE Sodium dodecyl sulfate- Polyacrylamide gel electrophoresis

SEM Standard error of the mean

siRNA Small interfering Ribonucleic acid

sh sh-RNA against SMPD1

shRNA Short-hairpin Ribonucleic acid

TAB TAK1 binding protein

TAK1 Transforming growth factor β activated kinase 1

TFs Transcription factors
TLR Toll-like Receptors

v/v Volume to volume w/v Weight to volume

WT Wild type (WT-SMPD1)

xg Times gravity

ABSTRACT

Niemann-Pick disease (NPD) types A and B are rare autosomal recessive diseases that are characterized by having decreased sphingomyelin phosphodiesterase 1 (SMPD1) activity. Patients suffering from this disease are unable to metabolize sphingomyelin and thus have a lack of ceramide. Ceramides are potent activators of p38α MAPK and are involved in cell signalling with bacterial infections. Increased susceptibility to respiratory bacterial infection is a known phenotype of Niemann-Pick disease types A and B, and therefore we want to elucidate how a decrease in SMPD1 activity may contribute to this disease. The overall goal of this project aims to explore SMPD1's role in defence against bacterial infection via activation of p38α MAPK by bacterial stimulation with Pseudomonas aeruginosa diffusible material (PsaDM). The scientific approach to examine this involves several methods, performed in human airway epithelial cells (AEC) exposed to bacterial stimuli. Stable AECs expressing a short-hairpin RNA (shRNA) against SMPD1 have been generated. The effects of SMPD1 knockdown using shRNA can be seen by comparison to cells without SMPD1 knocked down with respect to p38a MAPK phosphorylation and cytokine production. The basal level of activated p38α MAPK is elevated in AEC when SMPD1 is knocked down. Furthermore, various cytokines, in particular IL-8, have higher mRNA expression levels in SMPD1 knocked-down AECs. Finally, identification of potential binding partners was done by tandem affinity purification followed by mass spectrometry analysis. Understanding the role of SMPD1 in host defence mechanisms of the lungs is crucial to develop novel therapies aimed at improving the quality of life of patients suffering from NPD.

ABRÉGÉ

Les maladies héréditaires Niemann-Pick de type A et type B sont causées par une perte de la fonction de l'enzyme sphingomyélinase acide (SMPD1). Ce sont de maladies rares mais graves, et les infections pulmonaires contribuaient grandement à la morbidité et la mortalité des personnes atteintes. SMPD1 est une enzyme impliquée dans la conversion de la sphingomyéline en céramide dans les membranes cellulaires. La défense des voies aériennes contre l'infection bactérienne implique souvent l'activation de la protéine kinase p38α MAPK, une enzyme essentielle au système de défense immunitaire inné. Ce projet de recherche vise à comprendre le rôle de SMPD1 dans la réponse immunitaire innée des voies respiratoires aux infections bactériennes, stimulée par Pseudomonas aeruginosa (PsaDM). Nous examinons la réponse des cellules épithéliales aériennes (CEA) en mesurant l'activation de la MAPK p38α. Le niveau de base de p38α MAPK activé est élevé à CEA stables sans SMPD1. En plus, la voie MAPK p38α est impliquée dans la régulation de la synthèse des cytokines pro-inflammatoires. Diverses cytokines, notamment I'IL-8, ont des niveaux plus élevés d'expression de l'ARN messagers dans les CEAs sans SMPD1. Enfin, l'identification de partenaires de liaison potentiels a été réalisée par purification d'affinité en tandem suivie d'une analyse par spectrométrie de masse. Donc en mesurant l'effet de SMPD1 sur la phosphorylation de MAPK p38α et la production de cytokines pro-inflammatoire ca aidera à mieux comprendre son rôle face d'une infection.

CHAPTER 1: INTRODUCTION

1.1. Pertinent Respiratory Diseases

1.1.1. Niemann-Pick Disease and SMPD1:

Niemann-Pick Disease (NPD) is classified into 3 types: Type A, Type B, and Type C. Niemann-Pick disease types A and B are rare autosomal recessive diseases that are characterized by having decreased sphingomyelin phosphodiestase (SMPD)-1 activity (also known as acid sphingomyelinase, ASM), due to mutations in SPMD1 gene^{1,2}. Type C is classified by mutations in the Niemann-Pick C (NPC) 1 and NPC2 genes1. For the purpose of this thesis, we focus on SMPD1 and thus only Types A and B will be referred to when discussing NPD. This disease has a frequency of approximately 1 in 100,000 births and is more prevalent among the Askenazi Jewish population^{3,4}. While defects in SMPD1 lead to a systemic disease, children who suffer from this disease are more susceptible to respiratory infections which is the major cause of morbidity and mortality^{4,5}. SMPD1 is a lysosomal enzyme that converts sphingomyelin to ceramide at the cell membrane. In NPD, SMPD1 is nonfunctional and this results in an accumulation of sphingomyelin within the cell⁶. Under conditions of stress SMPD1 translocates from the lysoszome to the outer leaflet of the membrane resulting in production of ceramide⁷. This reaction involves cleavage of the phosphodiester bond of sphingomyelin and the release of phosphocholine in order to generate ceramide, an important molecule involved in several signalling cascades. Upon stimulation by bacteria, SMPD1 rapidly translocates to the outer leaflet of the cell membrane to initiate this conversion^{7,8}. Figure 1

demonstrates this process of membrane translocation of SMPD1. This process is mediated by exocytosis of lysosomes, which is dependent on intracellular Ca²⁺ levels^{7,9}. As a consequence of being a lysosomal protein, SMPD1 has an optimal pH of approximately 4.5¹⁰. Additionally, SMPD1 is recycled back into the cell through endocytosis via the mannose-6 phosphate receptor as demonstrated by the requirement of mannose-6-phosphate lysosomal targeting of the enzyme ^{7,9}

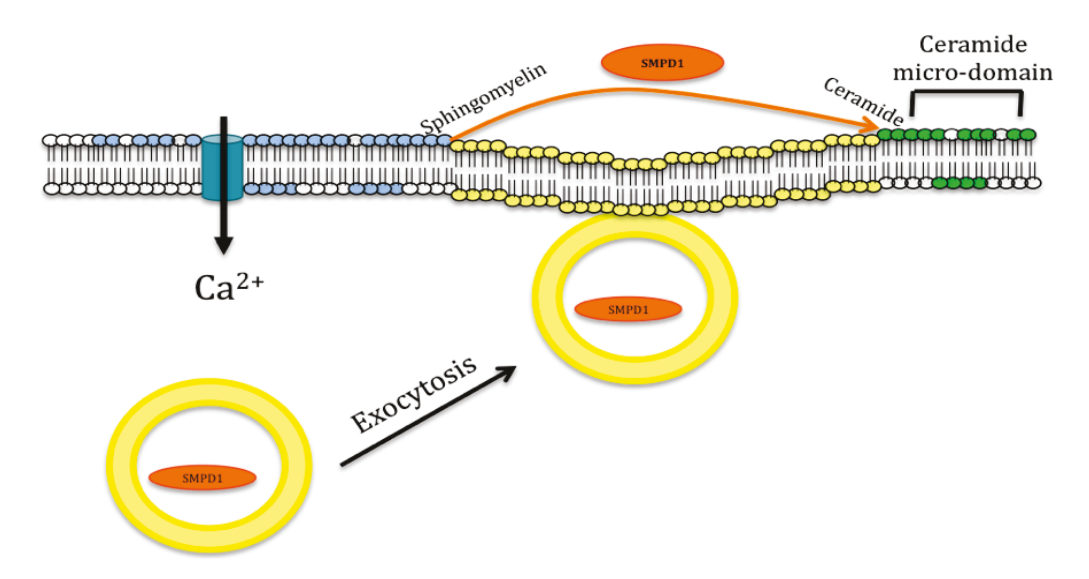


Figure 1: Translocation of SMPD1 from Lysosome to Outer-leaflet of Membrane to Produce Ceramide (Adapted⁷).

In mammalian cells, infection triggers SMPD1 activation, along with calcium influx, leading to the subsequent translocation of SMPD1 to the extracellular leaflet of the cell membrane, where SMPD1 is able to convert sphingomyelin to ceramide, resulting in ceramide micro-domains.

Patients with NPD have an accumulation of sphingomyelin in their tissues as a result of a dysfunctional SMPD1¹¹. Type A is categorized by severe neurological degeneration as well as delayed psychomotor development, and results in early childhood death of around 2 to 3 years of age^{1,2}. Type B manifests differently; it is a slow progressing visceral form with pulmonary involvement and non-neurological degeneration,

resulting in a longer survival time to adolescence or adulthood^{1,2}. Very little is known about the pulmonary implications of NPD.

Genetic mutations of NPD are constantly being revealed^{1,12,13}. Many patients show intermediate phenotypes of both Type A and B¹². SMPD1 is a 75 kDa prepropolypepeptide, and is processed into a 72 kDa form which is in turn cleaved into either its 57 kDa or 70 kDa form. The 70 kDa form is the functional enzyme, and the smaller form has no enzymatic activity¹⁴. Furthermore, both the mature form as well as it precursors have 6 potential N-glycosylation sites, as seen in Figure 2. It has been demonstrated that at least 5 of these are important for proper folding, protection against proteolysis and enzymatic activity^{14,15}.



Figure 2: Graphical Representation of Potential Glycosylation Sites (adapted¹⁵)

Representation of important domains and sites on SMPD1 protein for activity and proper functioning.

Ceramide itself is a key signalling molecule, and its absence will clearly result in many downstream effects. Additionally, having a decrease in SMPD1 activity has been linked to higher susceptibility to bacterial infection¹⁶ which is most likely due to dysregulation of the host's defense system and ability to fight off infection¹⁷. Another important aspect of ceramide is that it directly affects membrane rigidity. This is an important aspect for membrane turnover as well, in particular the generation of an acidic microenvironment that aids the enzyme in proper functioning¹⁸. Acidic microenvironments exist not only in lysosomes but also in domains

on the outer leaflet of the plasma membrane¹⁹. It is important to note that SMPD1 activity results in the formation of these microenvironments which are critical for the internalization of bacteria, such as *Pseudomonas (P.)* aeruginosa, into the cells as well releasing inflammatory cytokines⁹.

Finally, research has also been conducted on ASMKO mice (SPMD1 knockout mice)10,20,21. There are two different mouse models that were established at the same time, but independently of one another^{21,22}. Both of these mouse models exhibit phenotypes of NPD, however, they do vary to a certain degree in survival, as well as onset of symptoms¹⁰. Nevertheless, this research has demonstrated that the death of ASM deficient mice was caused by an exaggerated release of cytokines upon P. aeruginosa infection^{22,23}. Specifically, the infection of epithelial cells with P. aeruginosa triggers release of several pro-inflammatory cytokines, including IL-1^{23,24} and IL-8 which results in increased neutrophils recruited^{23,25}. This amplifies the inflammatory response leading to disease. Additionally, SMPD1 knockout mice were found to be resistant to several types of stress-induced apoptosis9. Furthermore, it is suggested that altering the sphingomyelin metabolism pathway causes a dysfunctional host response to bacteria, leading to chronic infection, and this is suggested to be due to effects on cell survival pathways¹⁷. In terms of pulmonary studies done on these mice, the research is fairly limited. There is evidence that SMPD1 is important to surfactant clearance in the lungs as total levels of surfactant lipid and protein were elevate in SMPD1 knockout mice²⁶.

Sphingolipids are clearly important with regard to cellular signalling in response to bacterial infections, which is why understanding the role of

SMPD1 and its link to innate immunity, in particularly host inflammation, is of significance.

1.1.2. Cystic Fibrosis:

Cystic Fibrosis (CF) is a hereditary disease whereby chronic respiratory bacterial infections lead to the major aspects of morbidity and mortality of the patients. This is an autosomal recessive disease, having a rate of incidence of 1/2913 births among the Caucasian population²⁷. Preliminary research in the early 1980s demonstrated that in CF, epithelial cells have a defect in ion transport, in particular chloride ion transport²⁸. Nine years later, the gene responsible for CF was discovered^{29,30}. Furthermore, the most common mutant allele was identified as the deletion of the 508th codon (Δ F508), resulting in deletion of a phenylalanine at that position, causing a malfunctioning of the intracellular processing of the CFTR protein³⁰. In airway epithelium, having a defective CFTR protein leads to mucus hyper-secretion and inflammation^{31,32}. Moreover, in CF patients, the lungs contain higher levels of pro-inflammatory cytokines, while simultaneously, lower levels of antiinflammatory cytokines³³. Altogether the defects of CF lead to chronic lung infection, due to hyper-inflammation, which consequently results in tissue damage. Eventually the outcome and overall impaired lung function can lead to death due to cardio-respiratory complications³⁴.

Numerous bacterial species are relevant to CF, however chronic *P. aeruginosa* infection is most prevalent, especially in older patients^{35,36}. A defect in CFTR facilitates the ability for bacteria to colonize and thrive, due to dehydrated mucous secretions which results in a thicker mucous layer in the lungs of CF patients, as well as a lower airway surface pH^{37,38}.It is

estimated that chronic infection with *P. aeruginosa* occurs in up to 85% of patients by the time they reach adolescence³⁶. This is extremely significant since this is highly associated with the hyper-inflammatory response and subsequent lung tissue damage.

Ceramide levels are increased in the lungs of CF patients^{39,40}. As discussed previously, ceramide is a key regulator in the inflammatory response. There are higher levels of IL-1 and IL-8 in the lungs of CF patients⁴¹. The accumulation of ceramide has been linked to this, in addition to increased neutrophils and macrophages in the lung⁴⁰. Several of the characteristic symptoms of CF are coupled to increased ceramide concentrations. These include not only chronic pulmonary inflammation and infections of *P. aeruginosa* but also death of epithelial cells⁴⁰. This has led to the possibility of treating CF by normalizing the levels of ceramide in patients by inhibition of SMPD1. It has been demonstrated in mice that long-term inhibition of SMPD1 corrects ceramide levels in CF mice, as well as minimizing inflammation and these mice are no longer more susceptible to pulmonary bacterial infection⁴². A possible method to achieve ceramide normalization in the lung is by use of small molecule inhibitors directed to SMPD1. In particular two drugs have been used to inhibit SMPD1 in hopes of normalizing ceramide levels and therefore diminishing CF symptoms and patients' susceptibility to respiratory bacterial infection to prevent mortality. The first of these molecules is amitriptyline; this was developed as a tricyclic antidepressant and was recently thought to be a safe and well tolerated treatment for CF patients, but is only effective in some patients⁴³. In another study, amitriptyline treatment restored normal ceramide levels as well as decreased

inflammation in the lungs, but there were widespread side effects associated with this treatment, such as undesirable effects on the cholinergic and histaminergic systems³⁹. Amitriptyline indirectly inhibits the functional mechanism of SMPD1, as it is able to insert into the inner leaf of the lysosomal membrane and subsequently cause membrane-associated enzymes, like SMPD1, to detach⁴⁴. The second drug is perhexiline, which also inhibits SMPD1 indirectly, but has not been tested in humans. Perhexiline is a calcium channel blocker, and calcium is needed to signal the translocation of SMPD1 from lysosome to outer-leaflet of membrane⁴⁵. However, calcium is required for numerous other cellular processes, and therefore the specificity of this drug is called into question.

Both CF and NPD are two fatal diseases involving genetic mutations causing imbalances in ceramide levels and metabolism. As a result patients have increased susceptibility to respiratory bacterial infections. Developing novel means to normalize ceramide levels in diseases like NPD and CF is a venue that is currently being explored. Therefore understanding the role played by SMPD1 in host defense mechanisms of the lungs is crucial to develop novel therapies aimed at improving the quality of life of patients suffering from CF and NPD.

1.2. Cell Signalling

1.2.1. Mitogen Activated Protein Kinases:

Mitogen Activated Protein Kinases (MAPK) are evolutionarily conserved protein kinases that play an essential role in the innate immune system reponse⁴⁶⁻⁴⁸. MAPKs are a group of serine/threonine protein kinases and are involved in various vital cellular processes. These

processes include: proliferation, cell differentiation, stress response, apoptosis, and immune defense^{49,50}. Additionally, MAPKs contain a dual phosphorylation motif, Thr-xxx-Tyr, which is a distinctive property^{46,51}. Dual phosphorylation of MAPK kinases (MKKs) can be activated by stress⁴⁶.

In mammalian cells, there are three major defined MAPK pathways. The first is the extracellular signal-related kinase (ERK) pathway. This pathway is mainly activated upon mitogens and growth factors and therefore is a key regulator in cell proliferation^{52,53}. The second is c-Jun amino-terminal kinases (JNK) pathway. JNKs are activated by a variety of stimuli, such as cytokines and growth factors, and once activated lead to the consequent activation of multiple transcription factors^{52,53}. Finally, there is the p38 pathway, of which there are 4 isoforms involved: α , β , γ , and δ . Activation of p38 is highly linked to both inflammatory cytokines and environmental stresses^{46,52}. It is suggested that once activated, p38 can translocate to the nucleus, as well as phosphorylate transcription factor and cytoplasmic targets⁵². MAPK pathways are activated by a cascade of sequential phosphorylations (Figure 3).



Figure 3: Simplistic View of the Cascade of Sequential Phosphorylations in MAPK Pathway

The phosphorylation of MAPKs results in the ability to phosphorylate downstream targets, like transcription factors, which allows for the regulation of genes involved in various cellular processes such as inflammation. Figure 4 below, shows that transforming growth factor β

activated kinase 1 (TAK1), a MAPKKK, is an important component of intracellular signalling in the host response to inflammation. TAK1 is able to be activated by cytokines and stress signals⁵⁴ and leads to nuclear factor kappa-light-chain-enhancer of activated B cells (NFκB) activation through lipopolysaccharide (LPS) stimulation⁵⁵. Furthermore, it is also involved in activating p38α and JNK in the presence of LPS and other proinflammatory stimuli⁵⁶.

Stimulation of pattern recognition receptors (PRR) activates MAPKs involved in the induction of inflammatory genes⁵⁷. It is important to note that certain pathogens have developed ways to alter activation of the MAPK pathway. For example, the release of proteases that are able to degrade factors that are required for signalling⁵². Overall, MAPK signalling is a highly interactive and complex network involving numerous molecules.

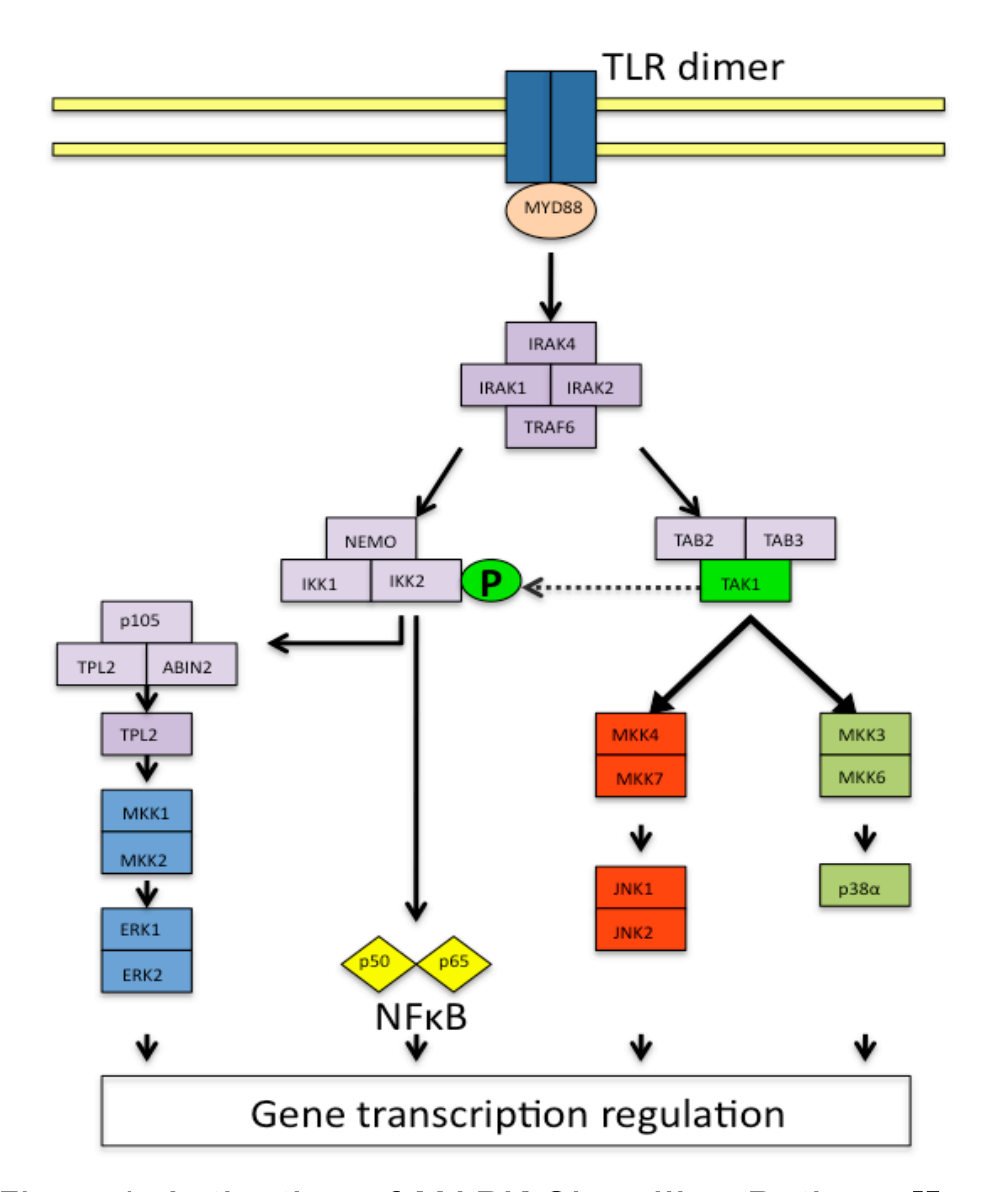


Figure 4: Activation of MAPK Signalling Pathway⁵⁷ Toll-like receptor (TLR) signalling, by dimerization of TLRs leading to activation of MAPKs and NF κ B is MyD88 dependent. Activation leads to regulation of gene transcription.

1.2.2. Airway Epithelial Cells:

Airway epithelial cells (AECs) function as a physical barrier between the external environment and the inner lung components. They play an essential role to protect the lungs both in a physical aspect as well as an immunological aspect. The airway epithelium is a complex structure lined by a continuous layer of epithelial cells⁵⁸. Figure 5 depicts the various cell types that can be found in the airways. The pseudostratified epithelium consists of basal cells, globlet cells, and ciliated cells^{58,59}. Each major cell type has a distinct histology as well⁵⁸. Furthermore, This is a very dynamic tissue in that it is constantly being renewed⁶⁰. It is important to note that both epithelial and innate immune cells are crucial components involved in the pathogenesis of respiratory diseases⁶¹.

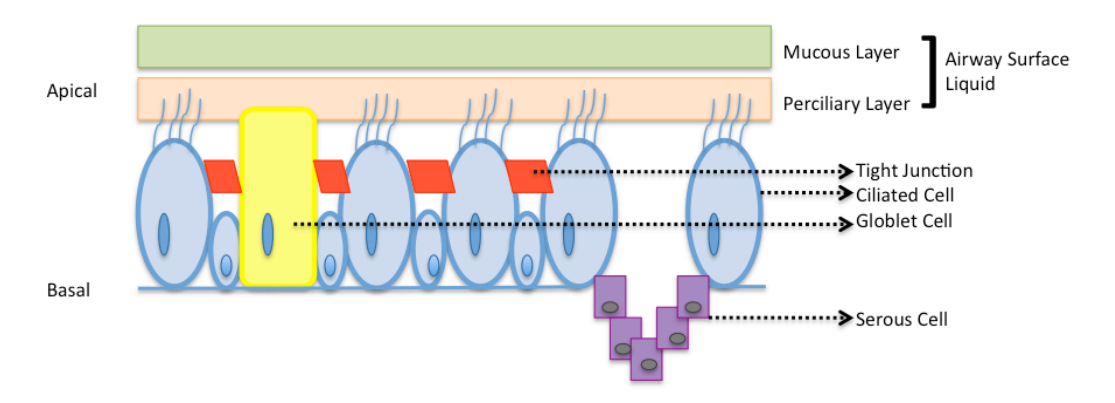


Figure 5: Pseudostratified Airway Epithelium 59,62.

Inflammation in the airways can be detrimental. Macrophages, epithelial cells and smooth muscle cells in the airways secrete various cytokines, in particular IL-1 and IL-8, in an acute inflammatory response⁶³. However, what is of great importance with respect to NPD and CF is chronic inflammation in the airways, which is a more complex process. Constant release of cytokines leads to increased number of neutrophils at the site of infection⁶³. This along with activation of T lymphocytes and eosinophil recruitment can lead to epithelial cell damage⁶³. Another important function of AECs is the clearance of environmental agents. This process is dependent on the thin mucous layer and its ability to clear particles by movement out of the lungs⁵⁸. Mucociliary clearance is aided

by the presence of surfactant as well as mucins, which are molecules that are effective for trapping particles and binding bacteria⁵⁸. Effective clearance is a vital process that is necessary for normal functioning of the airway epithelium.

Having a properly functioning airway epithelium is essential to generating a normal immune response to pathogens. Additionally, AECs and immune cells act together to protect airways and prevent disease⁶¹. AECs are early responders to pathogens and therefore direct the consequent immune response. As the first line of defence against microbes, the airway epithelium has developed means by which to recognize bacteria. AECs express a number of PRRs that are able to recognize bacteria and respond to pathogen associated molecule patterns (PAMPs), which consist of a variety of molecules and virulence factors⁶⁴. One of the best-characterized classes of PRR that are expressed in AECs are the Toll-like Receptors (TLR), which can recognize a number of different PAMPs to initiate the innate immune response.

1.2.3. Innate Immune Response Through TLR Signalling:

Innate immunity is essential to defend the lungs against pathogens and the TLRs are essential for recognition of PAMPs by the innate immune system. When pathogens bind to TLRs, this initiates a downstream signalling cascade that results in initiation of an inflammatory response. Signalling through this pathway involves recruitment of adaptor molecules, which in turn are able to generate the appropriate response. TLRs are expressed not only in immune cells but also in non-immune cells, such as epithelial cells⁶⁵. Currently there are 10 human TLRs, and

TLRs 1, 2, 4, 5, 6, 9 are associated with response to bacteria⁶⁶. TLR4 and TLR5 play a major role in controlling the replication of bacteria in the host in response to P. aeruginosa infection⁶⁷. TLRs respond to bacterial components to activate MAPKs and NFkB to induce cytokine production and neutrophil recruitment⁶⁸. All these steps are tightly regulated to necessitate an appropriate response to pathogens. Normal innate immune system's defense against bacterial infection involves activation of p38a MAPK. Therefore, to illicit a proper response to bacterial infection, proper activation of p38 α MAPK is necessary⁶⁹. p38 α MAPK is involved in directing cellular responses to a diverse array of stimuli, such as mitogens or cytokines in order to regulate proliferation, gene expression, differentiation, and mitosis. NFkB is a transcription factor involved in regulation of genes responsible for inflammatory response. Our lab has shown that p38α MAPK is activated in AEC by PsaDM stimulation, in particular through activation of TLR569. Figure 6 below shows a generalized schema of an appropriate response brought about by bacterial stimulation in AEC. The dimerization of TLRs leads to recruitment of adaptor molecules, such as MyD88 which subsequently results in the activation of four major signalling pathways: NFkB, ERK1/2, JNK, p38 α^{70} . Additionally, there is a MyD88-independent pathway that is beyond the scope of this thesis, however can affect p38 α MAPK and NFkB signalling⁶⁴.

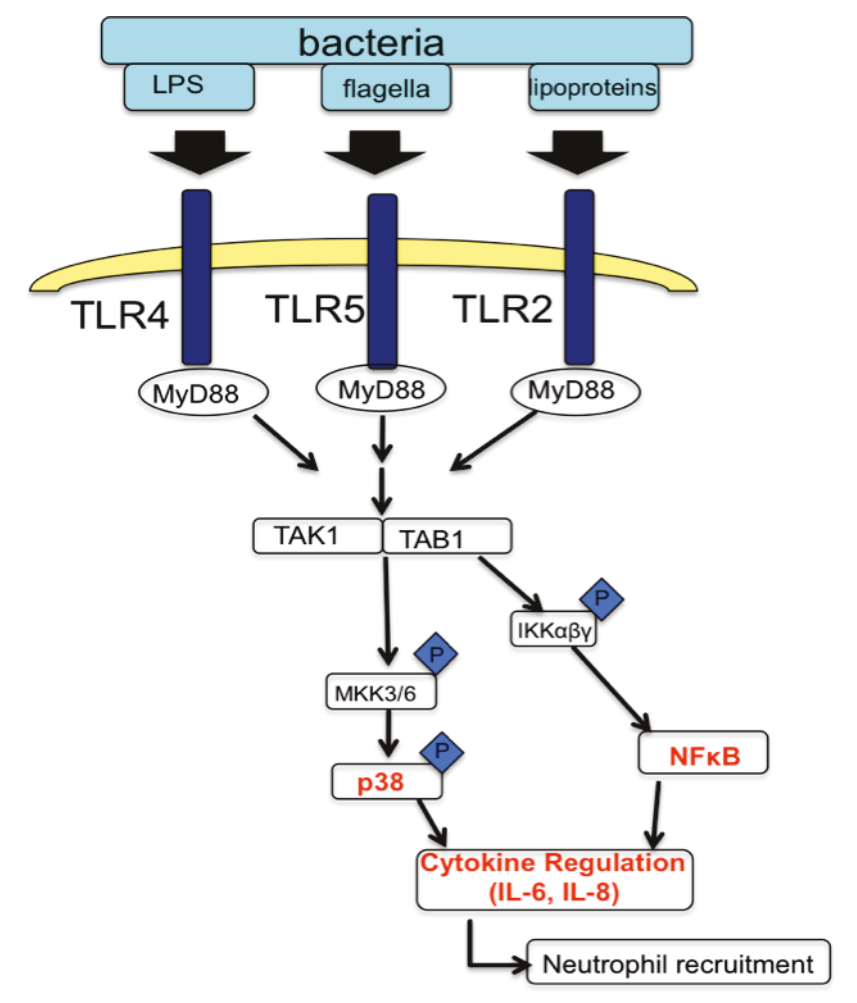


Figure 6: Normal innate immune system's defence against bacterial infection involves activation of p38 α MAPK through TLRs (adapted from 68)

1.2.4. NFkB Signalling:

PRRs also activate NFkB pathways, and together with activation of MAPKs, a proper immune response is achieved⁵⁷. This pathway is highly important in infections as it is considered a key modulator in the innate immune response⁷¹. Therefore, it is not surprising that this pathway and the proteins associated with it are highly conserved⁷². NFkB is a protein complex, consisting of homodimers or heterodimers that are able to regulate transcription. It has been established that there are five

mammalian NFκB proteins: p65 (RelA), RelB, c-Rel, p105/p50 (NF-κB1), and p100/52 (NF-κB2)^{73,74}. They all share a conserved Rel Homology Domain (RHD) which is essential for dimerization, as well as for DNA binding, lκB associations, and finally translocation to the nucleus in order to carry out its transcriptional regulation⁷⁴.

The canonical pathway provides sufficient means for understanding NF κ B signalling. The heterodimer involved in the canonical pathway is p65/p50 and is associated with the inhibitor of NF κ B proteins (I κ Bs), I κ B α 73 . The role of I κ B α is to sequester p65/p50 in the cytosol. Once the pathway is activated, for instance by an environmental stress such as bacterial pathogens, the I κ B kinase (IKK) complex becomes activated^{73,75}. IKK is an upstream kinase that phosphorylates I κ B α at 2 sites, Ser32 and Ser36, leading to degradation of the inhibitor by the proteosome as a result of polyubiquitination^{74,76}. This allows translocation of NF κ B into the nucleus where it is able to induce transcription. Once activated in the nucleus by phosphorylation, NF κ B binds to DNA with κ B-elements and regulates the transcription of various genes involved in an array of functions such as inflammation, immune response, proliferation and apopotis⁷³.

Deregulation of NFκB signalling has been associated with various diseases. In CF, IL-8, a neutrophil recruitment cytokine, has been shown to be elevated as a result of deregulation of NFκB signalling⁷⁷ Furthermore, inhibition of NFκB signalling by IKK inhibitors, resulted in decreased number of neutrophils in the airways⁷⁸. Only one study, 20 years ago, has published on NFκB signalling in the context of NPD⁷⁹. It was shown that NPD type A fibroblasts were still able to induce IL-8

expression through the NF κ B pathway, by stimulation with IL-1 and TNF α^{79} . This would indicate that SMPD1 activity is not essential for inducting IL-8 expression via the NF κ B pathway.

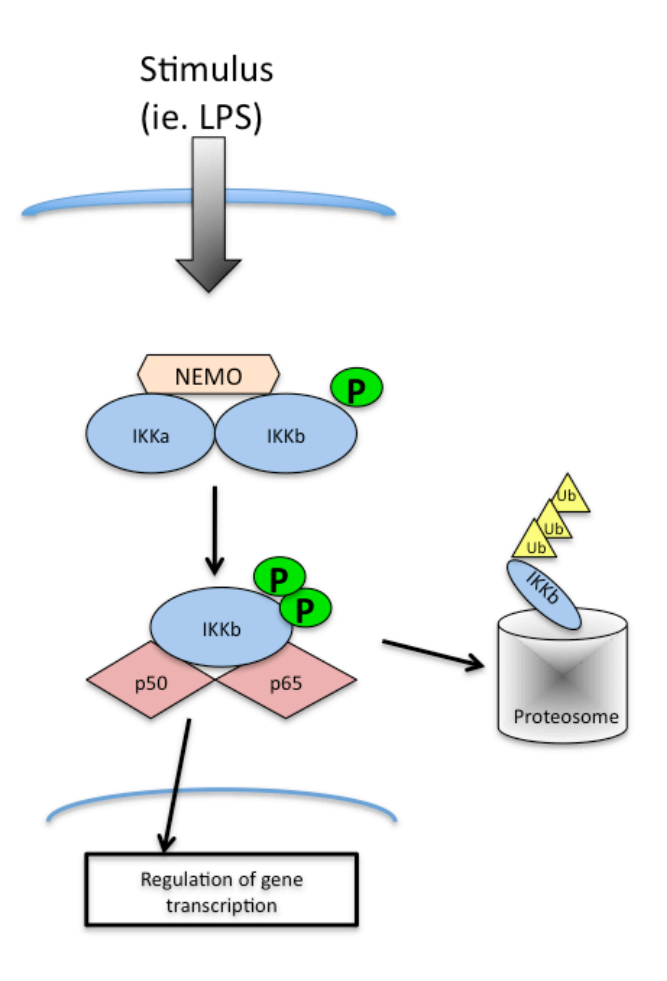


Figure 7: Canonical NFκB Signalling Pathway (adapted from⁷³)

1.2.5. Ceramide/Sphingolipid Pathway:

Lipids are organized in the cell membrane rather than being inserted in random formation. Sphingolipds are the major component of eukaryotic cellular membrane, in which sphingomyelin is the most abundant sphingolipid⁸⁰. Ceramide is a ubiquitously expressed second messenger, which is implicated in numerous signalling pathways that are

particularly sensitive to stress. Inflammation is strongly associated with ceramide concentration. Both ceramide and sphingomyelin concentrations have the tendency to be elevated in inflamed tissues¹¹. In the lungs, it is primarily C24 and C16 ceramides present, however the roles of these different ceramides has not specifically be explored⁸¹. Ceramide is generated from the hydrolysis of sphingomyelin or *de novo*, as seen below in Figure 8. The generation of bioactive ceramide from sphingomyelin is through the salvage pathway^{14,81}. Ceramide formed via the salvage pathway is by the activation of PKCδ. Phosphorylation of SMPD1 at serine 508 by PKCδ in the lysosome leads to its translocation to the cell membrane⁸².

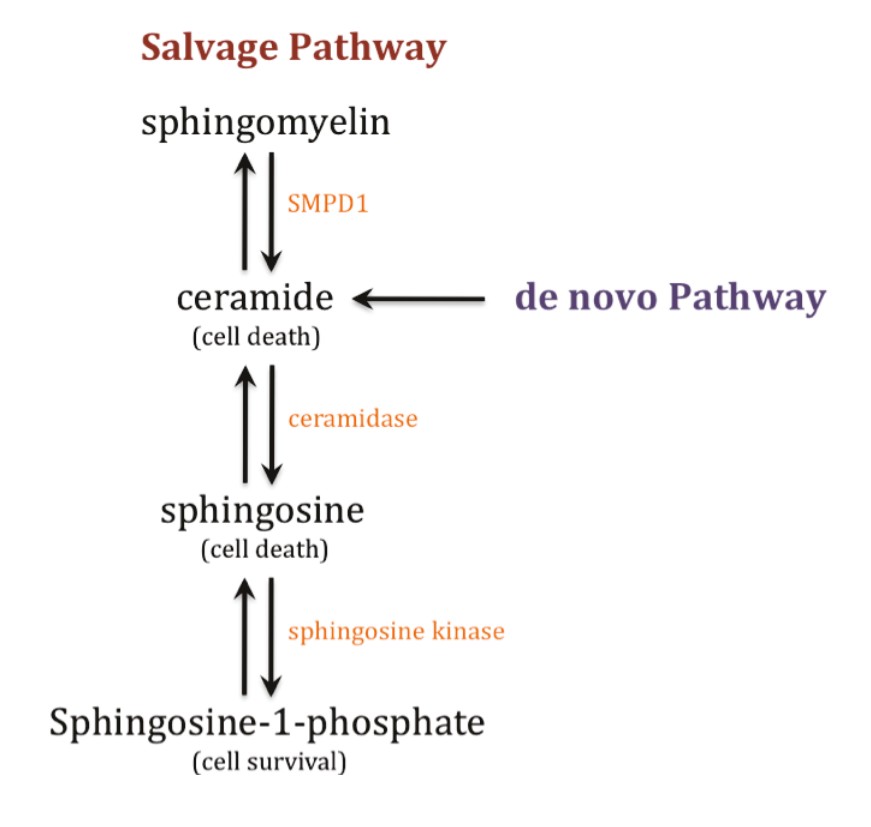


Figure 8: Sphingomyelin/Ceramide Pathway

This signalling pathway is vital for cells, as it has been shown that ceramide plays a key role in the induction of apoptosis from stress or from bacterial infection, such as from *P. aeruginosa*^{23,83}. SMPD1 is a known initiator of the sphingomyeline/ceramide signalling pathway with respect to stress stimuli¹⁰. Stress activates the rapid translocation of SMPD1 to the outer leaflet of the cell membrane to produce ceramide¹⁰. This results in the rapid production of ceramide, while the *de novo* pathway requires more time.

SMPD1 and ceramide have a crucial role in response to infection and host-pathogen interactions. Ceramides have a pro-oxidative role in inflammation and furthermore, ceramide is a known activator of p38α MAPK⁸⁴. Therefore, ceramide is important in cell transduction signalling involved in bacterial infection, such as for the internalization and elimination of bacteria, particularly in lung epithelial cells. SMPD1 knockout mice have been shown to be resistant to radiation and apoptosis⁸⁵. Research has shown that when C16 ceramide was added to SMPD1 knockout mice, this corrected defects seen in pathogen uptake, and apoptosis⁸³.

The generation of ceramide at the cell membrane, as a response to infection, leads to the development of ceramide-rich microdomains, or lipid rafts. These microdomains create changes in membrane structure and ultimately generate a local environment on the membrane. Moreover, these ceramide-rich microdomains are involved in the internalization of pathogens, such as *P. aeruginosa*, and have also been shown to control the release of cytokines in infected epithelial cells²³. Another important aspect of these microdomains is that they led to the reorganization of cell

membranes. For instance, ceramide-rich microdomains result in the clustering of receptors involved in apoptosis and therefore led to amplification of the signal⁸⁶. The formation of ceramide brings together signalling proteins to trigger downstream changes, allowing these ceramide-rich microdomains to trap and cluster receptor and signalling molecules¹⁹. Furthermore, they allow for enhanced density of signalling proteins at the membrane promotes receptor dimerization and facilitating protein-protein interactions⁹.

SMPD1 is an essential regulatory enzyme in ceramide homeostasis, demonstrated in Figure 8. The balance of these reactions coincide with the balance of anti and pro inflammatory cytokines. Ceramide accumulation is associated with cell death and induction of apoptosis, sphingosine is an apoptotic mediator and sphingosine-1-phosphate mediates transcriptional regulation of key targets for survival and proliferation⁸⁷. The balance of the molecules involved in ceramide metabolism play an important role in the determination of a cell's fate in the face of infection.

1.3. Signalling Involved with SMPD1 in Context of Innate Immunity

1.3.1. p38α:

p38α MAPK is strongly activated by environmental stresses as well as inflammatory cytokines, therefore this signalling pathway is important to the regulation of the biosynthesis of inflammatory cytokines. Bacterial infection and the subsequent inflammation involves an increase in phosphorylation of the p38α MAPK⁶⁹. Upon bacterial infection, epithelial

cells send distress signals by secreting cytokines, which are involved in neutrophil migration to the site of infections in a p38 α MAPK-dependent fashion⁶⁹. MKK3 and MKK6 are selective for p38 MAPK ⁴⁶. p38 α MAPK is a key mediator in the production of pro-inflammatory cytokines in AECs. Our lab has shown that in a cystic fibrosis model cell line, both p38 α and ERK are hyper-activated following bacterial challenge by PsaDM, and this results in higher IL-6 levels⁸⁸. Additional evidence demonstrates the role of p38 α in the biosynthesis of other cytokines such as IL-1⁸⁹, TNF α ⁸⁹, and IL-8⁹⁰. It has been shown that antioxidants block p38 α activation⁹¹. This is indicative of a possible role of ROS on p38 α , and subsequently on the production of IL8. It has also been shown that ceramide microdomains are critical in redox signalling to regulate apoptosis in alveolar macrophages when challenged with *Paeruginosa*⁹². However, SMPD1 was not required for p38 α MAPK signalling in SMPD1 knockout murine macrophages in response to TNF α stimulus⁹³.

The level of p38 α MAPK activation in AECs is critical as this is what determines the host's immune response. There is a threshold of p38 α activation necessary to prompt the host's response as a results of PsaDM stimulation⁶⁹. Since p38 α MAPK is not an isolated component of the MAPK signalling pathway, it is therefore under tight regulation. There are many upstream signals that converge and result in activation of p38 α 50. In human fibroblasts that are SMPD1 deficient, phosphorylation of p38 α MAPK was no different compared to normal human fibroblasts⁹⁴, yet in HeLa (Helen Larson cells, human uterine cervical carcinoma cells), inhibition of SMPD1 reduced p38 α MAPK activation⁹⁵.

1.3.2. Cytokine Production:

Another signalling pathway, apoptosis signal-regulating kinase 1 (ASK1), is also important in innate immunity. AKS1 is an evolutionarily conserved member of the MAPKKK family which is involves in JNK and p38α MAPK activation⁹⁶. Ceramide induces the ASK1-MAPK pathway⁸⁴. Additionally, ASK1 activation is necessary for pro-inflammatory cytokine production following activation of TLR4⁹⁶. Protein phosphatase 2A is activated by ceramide, which is involved in both NFκB and MAPK signalling⁹⁷. One research group has shown that ceramide is believed to play a role in down regulation of IL-8 expression, since IL-8 expression levels increased when protein phosphatase 2A was inhibited in respiratory epithelial cells⁹⁸. This results contradicts what is known about ceramide, in that it activates pro-inflammatory cytokines; however it reinforces the idea that the appropriate balance of ceramide and how it is formed, either *de novo* or through the salvage pathway, is important in dictating its role and consequently the signalling pathways implicated for a response.

Over-release of cytokines in SMPD1 KO mice after infection with *P. aeruginosa* was the major cause of mortality²³. SMPD1 knockout mice who were treated with C16 ceramide had their levels of cytokine release corrected⁸³. The association between the death of SMPD1 KO mice from over-production of cytokines in response to *P. aeruginosa* infection is not yet fully understood. It is believed that in epithelial cells, apoptosis serves to balance the local immune response and therefore prevent overshooting release of cytokines²³.

The role of SMPD1 in cytokine production has seldom been investigated. One group developed SMPD1 inhibitors and showed that

when SMPD1 was inhibited there was a decrease in IL-6⁹⁹ as well as other cytokine levels¹⁰⁰. Furthermore, it has also been show that p38α MAPK activation is involved not only in the production of IL-6 but also in its transcript stability⁸⁸. Finally, sphingolipids have been associated with the regulation of cytokines like IL-6 and CCL5. IL-6 was shown to be negatively regulated by SMPD1⁹⁵.

Cytokine regulation by SMPD1 in the literature has wide-ranging results. In fact, the role of SMPD1 may very well be cell-type specifc⁹⁵. There are conflicting views on SMPD1 and p38α MAPK as well, and it is suggested that depending on the pathway implicated to produce ceramide, it can influence its effects on p38α MAPK signalling and cytokine production. Therefore, it is important to comprehend SMPD1's role in the innate immune system with regard to MAPK signalling and consequent cytokine production in response to bacterial challenge. In the airways, the correct balance between pro and anti-inflammatory cytokines is essential.

1.4. Rational and Objectives

Niemann-Pick disease (NPD) types A and B are rare autosomal recessive diseases that are characterized by decreased sphingomyelin phosphodiesterase 1 (SMPD1) activity, associated with mutations in the *SPMD1* gene. Patients suffering from NPD are unable to metabolize sphingomyelin and thus lack ceramides. Ceramides play a role in cell transduction signalling mechanisms involved in stress and inflammatory responses. Increased susceptibility to respiratory bacterial infections is a major contributor to morbidity and mortality of patients suffering from NPD. Bacterial infection leads to an increase in phosphorylation of the p38α

MAPK, an essential enzyme in the innate immune system's response to bacterial infections. Furthermore, upon bacterial infection by PsaDM, epithelial cells send distress signals by secreting cytokines. Importantly, ceramides are known agonists of p38α MAPK.

We hypothesize that SMPD1 plays a crucial role in regulation of the defense against bacterial infection through signalling via the p38α MAPK pathway. The objectives of my studies are three-fold: (1) to examine whether SMPD1 is involved in the activation of p38α MAPK in response to bacterial infections, (2) to understand the role of SMPD1 in the production of cytokines, and (3) to explore the overall function of SMPD1 in innate immunity. SMPD1 is known to have a role in uptake of pathogens, induction of apoptosis and cytokine release upon infection with *P. aeruginasa,* but the extent to which SMPD1 is involved is not yet that well understood. Overall, this research will help to better understand the role played by SMPD1 in host defense mechanisms of the lungs, which is crucial to develop novel therapies aimed at improving the quality of life of patients suffering from Niemann-Pick Type A and B disease.

CHAPTER 2: Materials and Methods

2.1. Materials

For cell culture the following antibiotics used were: Penicillin-Streptomycin, Hygromycin, Blasticidin, Zeocin and Genticin as described and purchased from Invitrogen (Burlington, ON.). Additionally, Dulbecco's Modified Eagle Medium (DMEM) with 4.5 g/L D-glucose was purchased from Invitrogen. Agonists used include: H₂O₂ (Sigma-Aldrich, Oakville, ON.), Sphingosine-1-phosphate (provided by Dr. James Martin's Lab Meakins Christie Research Institute, Montreal), and PsaDM which is produced in our laboratory. The inhibitors used include: 150mM Amitriptyline (Sigma-Aldrich), 10mM Perhexiline (Sigma-Aldrich), and BIRB0796 (kindly provided by Professor Sir Philip Cohen University of Dundee, UK). The plasmids that were used for transfections were prepared in the lab and are as follows: WT-SMPD1_pCMV4a, L225P-SMPD1_pCMV4a, WT-SMPD1_pcDNA5/FRT, L225P-SMPD1_pcDNA5/FRT, shRNA-NT_pSingle-TTS, shRNA-SMPD1_pSingle-TTS, and pFRET-HSP33. The reagents for transfections needed were: PEI reagent, TurboFect (Thermo Scientific, Rockford, IL, USA), and doxyxcycline to induce expression of sh-RNA (Clontech (Mountain View, CA, USA)).

2.1.1. Preparation of *P. aeruginosa* diffusible material

P. aeruginosa diffusible material was prepared by growing P.aeruginosa in 5 mL of desired media in 12 mL test tubes at 37°C for 72 hrs with shaking at 250 RPM. This was pelleted by centrifugation at 2100xg for 20 min. The supernatant was filtered through a 0.22 μm filter

(Millipore), aliquoted and stored at -20°C. Aliquots were heat inactivated for 10 min at 95°C prior to stimulating cells.

2.2. Methods

2.2.1. Cell Culture

Immortalized human bronchial epithelial cells (BEAS-2B) were purchased from ATCC (Rockville, MD, USA). BEAS-2B were maintained at 37°C, 5% CO₂, 100% humidity in DMEM. Both 10% v/v heat inactivated fetal bovine serum (FBS), and 100 μg/mL Penicillin-Streptomycin (P/S) were added to medium. For experiments with sh-RNA knockdown cells, doxyclycline was added to medium at 5μM concentration. Cells were grown to confluence in a 12-well plate (Sarstedt, Montreal, Quebec) in 1.0 mL of media, and either transfected or treated with agonists prior to analysis. Human Embryonic Kidney (HEK) 293 cells were provided by Dr. Elizabeth Fixman's lab (Meakins-Christie). These cells were cultured at 37°C, 5% CO₂, 100% humidity in DMEM. Both 10% v/v heat inactivated FBS, and 100 μg/mL P/S were added to medium.

2.2.2. Construction of Flp-IN cells

Using HEK Flp-IN (Invitrogen) cells, novel constructs were generated in the lab. These cells were maintained at 37°C, 5% CO₂, 100% humidity in DMEM with 10% v/v heat inactivated FBS, 100 μg/mL P/S, 100μg/mL blasticidin, 15μg/mL hygromycin and 200 μg/mL zeocin were added to medium. The Flp-In system involved designing primers (Table 1) to insert WT and L225P SMPD-1 into pcDNA5/FRT Expression Vector. This allows for WT and L225P to have GFP and TAP tags (Figure 5).

Construction of these vectors involved: Amplification of the gene of interest (WT and L225P SMPD1) using the following reaction: 100ng DNA, 5ul buffer, 5μL dNTPs, 2.8μL H₂O, 1.5μL of 10 μM forward primer, 1.5μL of 10 μM reverse primer, 1μL polymerase. A PCR was run using a temperature gradient, followed by purification of the PCR product. This product was used for restriction digests using Notl restriction enzyme. Following digestion, the product was ligated into the vector and purified. This was followed by mini-prep and maxi-prep of plasmid using commercial kits (Invitrogen). To prepare the HEK-Flip-In cells with the desired construct: 2.5 X 10⁵ cells per well were plated in each well of a 6 well plate in DMEM (no supplements). The following day these cells were transfected with a ratio of 7 Plasmid DNA: 1 Insert DNA (1.75 pOG44 and 0.25μL WT or mutant plasmids) and 4μL PEI in 100μL DMEM. These were incubated overnight to allow uptake of DNA after which media was replaced with DMEM with or without supplements and let to grow 1-2 weeks. Cells where then transferred to 12 well plate pre-coated with Purcol with DMEM only, and allowed to attach for 5 hrs. Media was then changed to Flip-INs medium (DMEM, 10% v/v heat inactivated fetal bovine serum (FBS), 100 μg/mL streptomycin (P/S), 100 μg/mL blasticidin, 15 μg/mL hygromycin). These stable cells allow for the inducible expression of WT and L225P following exposure to doxyxcycline. Once these Flp-In cell lines were produced, the TAP and IF experiments were conducted in these cells.

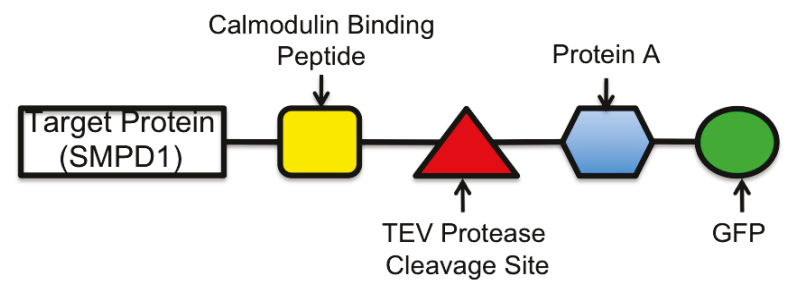


Figure 9: TAP Tag in HEK-Flp-In Cells

Table 1: Primers for Flp-In System

	Sequence (5'-3')
SMPD1-NotI-Foward	TTGCGGCCGCCATGCCCCGCTACGGAGCTCA
SMPD1-NotI-Reverse	TTGCGGCCGCCTAGCAAAACATGGCCTTGGCCA

2.2.3. Creation of stable BEAS-2B with shRNA to SMPD

BEAS-2B cells were transfected using the Knockout Inducible RNAi System (Clontech). The manufacturer's protocol was followed¹⁰¹. This system is made to provide an on/off control of shRNA by doxycycline. The primers that were designed are listed below and were at position 2157 of SMPD1 variant 1 sequence (NCBI). This was followed by plasmid purification for transfection. Once transfected, cells were selected with G418 at 600ug/mL. Cells were sorted into a 96-well plate, and when cells were confluent, they were split into a 12-well plate, then 6-well plate. Cells that expanded accordingly were screened and stocks were frozen. The stable cell lines that were created are: NT (non-target shRNA) and sh (shRNA for SMPD1).

Table 2: Primers for shRNA Knockdown

SMPD1-	tcgagGCAAGATCATCCGGTGAAATTCAAGAGA
shRNA top	TTTCACCGGATGATCTTGCTTTTTTACGCGTa
SMPD1-	agcttACGCGTAAAAAAGCAAGATCATCCGGTG
shRNA low	AAATCTCTTGAATTTCACCGGATGATCTTGCc

2.2.4. Cell Lysis and Immunoblot

After desired treatments, cells were removed from incubator, and washed twice with ice-cold phosphate buffered saline (PBS), which was then aspirated. Cells were lysed, on ice, with cold lysis buffer (50 mM Tris-HCl pH 7.5, 1 mM ethylene glycol tetraacetic acid (EGTA), 1 mM ethylenediaminetrtraacetic acid (EDTA), 1% (v/v) Triton X-100, 1 mM Sodium orthovanadate, 5 mM Sodium pyrophosphate, 0.27 M Sucrose, cOmplete-Mini protease inhibitor cocktail (Thermo Scientific) and 2 mM DTT. Cells were then scraped and samples spun down at 12,000 x g at 4°C for 5 min. Protein concentration was quantified by Bradford method, while 30µl of supernatant was added to 10µl of 4X loading buffer (0.24 mM Tris-HC, 8% sodium dodecylcsulfate (SDS), 40% glycerol and 36% distilled water) with 1X TCEP. Protein samples were heated at 95°C for 5 min, prior to loading 20µg of protein per sample onto 10 % Pro-pure Next Gel (Amresco, Ohio, USA). After running the SDS-PAGE (10 min at 80 volts then 1 hr 20 min a 120 volts), proteins were transferred to nitrocellulose membrane with cold transfer buffer for 35 min at 100 volts. The proteins were then transferred from the gel to a nitrocellulose membrane using ice-cold transfer buffer for 35 min at 100 Volts. Membranes were then blocked for 1 hr at room temperature or overnight at 4°C in 3% bovine serum albumin (BSA). Primary antibodies of interest were applied (Table 2) in 1% BSA in Tris-buffered saline containing 0.05% Tween-20 (TBST) and left overnight to incubate at 4°C. The primary antibodies were washed 3 times with TBST, and then membrane was incubated with secondary antibodies of goat anti-rabbit IgG (DyLightTM800) and goat anti-mouse IgG (DyLightTM680) at a dilution of 1:15000 for 45 min in the dark. Finally, membranes were washed 5 times with TBST, and a final rinse with PBS before scanning the membranes and quantification by Licor Odyssey imaging system. Analysis as conducted by taking a ratio of band intensities with respect to GAPDH or in the instance of examining phosphorylation, with respect to total protein.

Table 3: Antibodies For Immunoblots

Antibody	Dilution	Company
ASM (SMPD1)	Rabbit Polyclonal; 1/500	Santa Cruz Biotechnology
GFP	Rabbit Polyclonal; 1/1000	Santa Cruz Biotechnology
GAPDH	Mouse Monoclonal; 1/4000	Millipore
ERK1/2	Mouse Monoclonal; 1/1000	Cell Signalling
Phospho-ERK1/2	Rabbit Monoclonal; 1/1000	Cell Signalling
JNK	Rabbit Polyclonal; 1/1000	Cell Signalling
Phospho-JNK	Rabbit Polyclonal; 1/1000	Cell Signalling
ρ38α	Mouse Monoclonal; 1/1000	Cell Signalling
Phospho-p38α	Rabbit Polyclonal; 1/1000	Millipore

2.2.5. Cell Survival

Once cells are confluent they were treated (ie. H2O2, antibiotics) for a predetermined time period in order to determine cell viability by Trypan Blue Assay. Cells were collected after trypsinization, spun down at 0.8 RCF for 5 min. then the trypsin was aspirated. Cells were resuspended in medium, and $20\mu L$ of cells were taken to mix with $20\mu L$ of Trypan Blue (Sigma), and allowed mixture to incubate for 3 min. $10\mu L$ of this mixture was used to count on hemacytometer, where blue cells (stained) are nonviable and white cells (unstained) are viable. To calculate percent viable: (white cells per mL/(white cells per mL+blue cells per mL))x100.

2.2.6. ELISA (Enzyme Linked Immunosorbent Assay)

ELISA experiments were performed using a Human IL-8 kit purchased from Preprotech (Lot# 0610018). Supernatants were collected after stimulation of cells for 6 hrs with PsaDM and samples were diluted 1:10 before using 100μL for ELISA. Quantification was carried out according to the protocol provided by the manufacturer.

2.2.7. SMPD1 Enzyme Activity Assay

Cells were grown to confluence and lysed in the same manner as described in immunoblots. Protein concentration was determined by Bradford method. Protein samples (450µg/mL) were incubated with 15mM 2-N-hexadecanoylamino-4-nitrophenylphosphoryl-choline (Cedarlane, Burlington, On.) and 250nM sodium acetate buffer at pH 5.6 at 37°C for 4 hrs. 0.4 mL of stop solution (0.1M glycine, 0.1M NaOH at pH 10.5, 50%

ethanol) was added to the mixture and the OD at 410nm was read to determine the activity of SMPD1.

2.2.8. FRET

The HSP-FRET ROS probe ¹⁰² was transfected into Non-Target and sh-SMPD1 cells. Transfection was carried out overnight at 37°C using TurboFect (Therno Scientific) as per manufacturer's protocol. The following morning, plates were removed from incubator, cell medium was aspirated, and cells were scraped in 100μL PBS at room temperature and transferred in to microfuge tubes. Samples were centrifuged at 12,000 x g for 5 min, and pellets were resuspended in 400μL PBS. 100μL aliquots of samples were transferred into a 96-well plate, and were either left untreated or treated with 4mM H₂O₂ just prior to recording FRET. HSP-FRET was excited at 430nm and fluorescence emission was obtained at 470nm using the Tecan Infinite M1000 plate reader, heated to 37°C. The readings were taken at 3 min intervals, for 15 cycles.

2.2.9. Immunofluorescence

Hek-Flp-IN WT and L225P cells were plated in separate wells of a 12-well (Sarstedt) plate, with a 10mm diameter glass cover slide (Fisher Scientific, Fair Lawn, NJ, USA) inserted on the bottom of each well. After treatment of Hek-Flp-IN WT and L225P cells, the media was aspirated and cells were fixed by carefully placing 400μL of ice cold methanol into each well, and placing the plate at -20°C for 10 min. Methanol was aspirated and cells were carefully washed with PBS. Cells were permeabilized with 0.5% Triton in PBS for 5 min, then washed twice with

PBS and blocked in 5% BSA for 1 hr. Alexa568 Phalloidine (Invitrogen) was added at a 1:500 dilution (0.67 μ g/mL) in PBS, in the dark and humid environment. After 40 min, Hoescht (Sigma) was added at a 1:2000 dilution (5 μ g/mL), and incubated for remaining 5 min. Finally, slides were washed 3 times with PBS. Slides were then dried and mounted by Permafluor aqueous mounting media (Thermo scientific), and stored at 4°C. Slides were analyzed at 200X magnification through Olympus BX51 filters, using Image Pro 7 software to obtain images.

2.2.10. Tandem Affinity Purification (TAP)

Using Hek-Flp-In cells that were developed with the TAP affinity epitope tag, TAP was carried out using an adapted protocol¹⁰³. Briefly, cells were plated in 10cm cell culture dishes (Sarstedt), 3 per condition (untreated or PsaDM stimulated). After plating cells, doxycycline was added to the medium at a concentration of 500ng/mL and cells were grown to confluency. Cells were treated with PsaDM for 1 hr or left untreated. Cells were then scraped in 500µL of ice cold PBS, collected into microfuge tubes and pelleted by centrifugation at 500 x g for 5 min at 4°C. Supernatant was discarded, pellet was washed twice with ice-cold PBS and centrifugation was repeated. Cells were resuspended in ice-cold lysis buffer (50 mM Tris-HCl pH 7.5, 1 mM EGTA, 1 mM EDTA, 1% (v/v) Triton x-100, 1 mM Sodium orthovanadate, 5 mM Sodium pyrophosphate, 0.27 M Sucrose, Complete- Mini protease inhibitor cocktail and 2 mM DTT) and transferred to a pre-chilled Dounce homogenizer. Cells were homogenized with 25 strokes and incubated on ice for 5 min. This was repeated twice. Cells were then centrifuged for 10 min. at 12,000 x g at 4°C, and the supernatant was kept on ice. While centrifuging samples, 100μL of IgG Sepharose 6 Fast Flow beads (GE Healthcare) were washed with lysis buffer twice by centrifuging at 12,000 x g for 1 min. The beads were resuspended in 100µL lysis buffer. These beads were added to the cell extract (saved supernatant), and incubated for 2 hrs at 4°C on a rotating wheel. Next, beads were washed with ice-cold lysis buffer, then lysis buffer without inhibitors, then once with TEV cleavage buffer (10mM) Tris pH 8.0, 150mM NaCl, 10% v/v glycerol, 0.1% v/v NP-40, 0.5mM EDTA, 1mM DTT). Beads are then resuspended in 200μL ice-cold TEV cleavage buffer and 4µL AcTEV protease (Invitrogen) was added. Samples were incubated at 4°C overnight on rotating wheel. The following day, 50µL Calmodulin Sepharose 4B (GE Healthcare) beads were washed with calmodulin binding buffer, and resuspended in 50μL calmodulinbinding buffer (10mM beta-mercaptoethanol, 10mM Tris pH 8.0, 150mM NaCl, 10% v/v glycerol, 0.1% v/v NP-40, 1mM imidazole, 1mM Mgacetate, 2mM CaCl₂). Then the samples were incubated overnight and centrifuged at 12,000 x g for 5 min at 4°C. The eluate was collected in a new microfuge tube and CaCl₂ was added to a final concentration of 3mM. This was then added to the calmodulin beads and incubated for 2 hrs at 4°C on a rotating wheel. Beads were washed with ice-cold calmodulin buffer, then twice with ice-cold calmodulin buffer-2 (1mM β mercaptoethanol, 10mM Tris pH 8.0, 150mM NaCl, 1mM Mg-acetate, 2mM CaCl₂). The beads were mixed with 1X loading buffer with TCEP, and heated at 95°C for 5 min. Samples were centrifuged at 12,000 x g for 1ie, and then supernatant was loaded onto 10% Pro-pure Next Gel for a SDS-PAGE.

2.2.11. Mass Spectrometry

After performing TAP, and subjecting samples to SDS-PAGE, gel was washed with high performance liquid chromatography (HPLC) grade water. The gel was silver stained as described. Gel was fixed (50% methanol, 10% acetic acid) for 30 min, fixing agent was removed and fixation was repeated for 2 hrs. The gel was then rinsed with 20% ethanol for 20 min, followed by 20 min rinsing in water. The gel was reduced with sodium thiosulfate (Sigma) at 0.2g/L for 2 min. The gel was rinsed twice with water for 20 s, then incubated with silver nitrate (Lab Chem Inc., Pennsylvania, USA) at 2g/L for 30 min, and then rinsed once with water for 20 s. Finally, the gel was developed with 150mL of developing solution (30g/L sodium carbonate, 0.1% formaldehyde, 10mg/mL thiosulfate) for 2 min and the reaction was stopped by exchanging the developing solution with 1% (v/v) acetic acid, and then incubated for 30 min. When staining was complete, an image was immediately obtained with exposure of 15 s. Once image was obtained, gel was soaked in HPLC grade water for 30 min. Bands were excised using a sterile scalpel, and placed into microfuge tubes, which had been rinsed 3 times with 50%ACN/H2O solution. Bands were stored at -80°C, and then brought to the Institut de Recherche Cliniques de Montreal (IRCM) where samples underwent LC/MS/MS analysis followed by protein database search in NCBInr. Analysis of subsequent data was carried out using Scaffold Viewer and PANTHER Classification System 9.0.

2.2.12. NFkB Reporter Assay

The NFkB reporter cell line was created in the lab by stably transfecting pGL4.28 NFkB into BEAS-2B cells. These cells are grown in DMEM supplemented with 200µg/mL of hygromycin. To carry out the assay, cells were plated in 12-well plates (Sarstedt) until confluent, deprived overnight with Cnt-17 medium, then transfected with WT and L225P SMPD1 plasmids with PEI, and stimulated with PsaDM. After stimulation cells were washed twice with PBS then scraped in 45µL 1X Reporter Lysis Buffer (Promega, Madison, WI,USA) and collected in microfuge tubes. Samples were spun down at 12,000 x g for 5 min. For the reporter assay, 20μL of the samples were added to 96-wel plates and 25μL of luciferase assay reagent (20 mM Tricine, 1.07 mM (MgCO₃)·4 Mg(OH)₂·5H₂O, 2.67 mM MgSO₄, 0.1 methylenediaminetetraacetic acid, 33 mM dithiothreitol, 270 µM coenzyme A, 0.477 mM D-luciferin, and 0.533 mM adenosine triphosphate) was added to each well via an automatic injector. Finally, the Tecan Infinite M1000 plate reader recorded emission units.

2.2.13. Neutrophil Migration Assay

BEAS-2B AEC Non-Target and sh-SMPD1 cells were cultured and stimulated with heat inactivated PsaDM for 3 hrs. Cells were washed and placed in DMEM (no supplement) medium and incubated overnight. The medium was then collected, and hereafter referred to as: conditioned medium (CM). 600μL of this medium was placed in the bottom chamber of a transwell plate (Transwell with 5 μm pores, Costar, Montreal, Quebec) and 100μL of neutrophil cell suspension ((0.5x106 cells/well) in DMEM (no

supplement) obtained from Dr. Powell's Lab, Meakins Christie Research Institute) was placed into the upper chamber. After an overnight incubation at 37°C, the number of neutrophils that crossed the membrane into the bottom chamber was counted by a hemacytometer.

2.2.14. RNA Isolation and cDNA Synthesis

Total RNA was extracted after treatment of cells by the Trizol method (Invitrogen), following the manufacturer's protocol. Briefly, 0.5mL of Trizol was added per well, and cells were collected in a microfuge tube. Then 100 µL of chloroform was added, samples were shaken for 3 min then centrifuged at 12,000 x g at 4°C. The aqueous phase was pipetted into a new microfuge tube, while the organic layer was discarded. Next, 0.5mL of 100% isopronaol was added. To precipitate the RNA, samples were left on bench to incubate 10 min. This was followed by 10 min centrifugation at 12,000 x g at 4°C. The supernatant was decanted and the RNA pellet was washed with 0.5mL 75% ethanol, and vortexed briefly, then centrifuged for 5 min at 12,000 x g at 4°C. The supernatant was once again decanted and the remaining ethanol was removed. The pellet was left to dry, and once dried, 10μL of RNase-free water was added. Samples were vortexed and placed on ice for 10 min, then heated for 10 min at 65°C, then stored on ice. Quantification of total RNA was done using a NanoDrop. Once RNA was extracted by the Trizol method, 500ng total RNA was treated with 0.5µl DNasel (Thermo Scientific) and 1X DNasel buffer (Thermo Scientific). Samples were incubated for 30 min at 37°C. The reaction was stopped using 1µL of 50mM EDTA and a 10 min incubation at 65°C. Reverse transcription was carried by adding 9μL of RT-mix to each sample (1 μ L of 10mM random primers, 1 μ L of 10mM dNTPs, 4 μ L of 5x RT Fermentas Buffer, 0.5 μ L ribolock RNase inhibitor, 0.25 μ L Maxima RT, 2.25 μ L RNase-free water). Samples were placed in PCR and cycled at: 10 min at 25°C, 30 min at 50°C, and 5 min at 85°C. The resulting cDNA was diluted 1:20 with RNase-free water, and stored at -20°C.

2.2.15. Quantitative PCR

Semi-quantitative real-time PCR (qPCR) was performed in 96 well plate format using SYBR Green (BioRad) based detection on a Step-One-Plus machine (Applied Biosystems) with each 10 µL reaction containing approximately 100ng cDNA in 2.5µL, 0.3 µM of sense and antisense primers and 1X SYBR Green. The plate was sealed and cycled under the following conditions: 95°C for 10 min, 50 cycles of 95°C for 10 s and 60°C for 45 s. For quantification, mRNA levels of the housekeeping gene glyceraldehyde-3-phosphate dehydrogenase (GAPDH) were used for normalization and fold induction was determined from Ct values using Pfaffl method.

Table 4: Primers for qPCR

Gene	Forward Primer (5'-3)
CCL-1	ATGCAGGTACCCTTCTCCAG
CCL-12	ACAACTTTCTCCGCTTCGTT
CCL-13	CCAGAAGGCTGTCATCTTCA
CCL-20	GCAAGCAACTTTGACTGCTG
Eotaxin-1	AATCACCAGTGGCAAATGTC
GAPDH	AGCAATGCCTCCTGCACCACC
GM-CSF	ACTACAAGCAGCACTGCCCT
GRO-α	AGGGAATTCACCCCAAGAAC
IL-1β	CCCAACTGGTACATCAGCAC
IL-6	GTGTGAAAGCAGCAAAGAGG
IL-8	GTGCAGTTTTGCCAAGGAGT
IL-18	ATGGCTGCTGAACCAGTAGA
RANTES	GAAGCCTCCCAAGCTAGGAC
SMPD1	TCTATTCACCGCCATCAACC

2.2.16. Statistical Analysis

Statistical analysis was performed using GraphPad Prism 6 software. One-way analysis of variance followed by a multiple comparison test (Bonferroni) was used to test differences between groups. Also, two-way analysis of variance was used for grouped data, followed by a multiple comparison test (Bonferroni). Any p value < 0.05 was considered significant.

CHAPTER 3: Inhibition of SMPD1 Disrupts MAPKs and NFκB Signalling Pathways

3.1. Rationale

Previous work in our lab has shown that *Pseudomonas aeruginosa* diffusible material (PsaDM) is able to activate p38α MAPK^{69,104} and ERK1/ERK2¹⁰⁵ via the TLR pathway in AECs. This occurs predominantly through activation of TLR5 and TLR2. The main focus of the lab is on mechanisms and signalling involved in bacterial-driven inflammation and the host response, mainly in the context of cystic fibrosis. In response to PsaDM challenge, cells lacking CFTR (CFTRΔF508) exhibit a hyperactive p38α and ERK1/ERK2 MAPKs response⁸⁸.

However, it is not well known whether bacterial-driven inflammation is affected by loss of SMPD1 activity in airway epithelial cells. Specifically, examining p38 α MAPK, as it plays a prominent role in pro-inflammatory cytokine production upon bacterial infection, and SMPD1 as a potential upstream activator of p38 α MAPK.

Additionally in the CFTR∆F508 AECs, it has been established that these cells has lower levels of extracellular glutathione and are more sensitive to ROS88. In inflammation, ROS are important in signalling

molecules. This is why in addition to all the other aspects investigated in this thesis, ROS may also be implicated.

3.2. The impact of pharmacological inhibition of SMPD1 is ambiguous concerning the phosphorylation of p38 α

Initially, p38 α MAPK activation was examined in the presence of SMPD1 inhibition, using pharmacological inhibitors. Two inhibitors, perhexiline and amitriptyline were used to inhibit SMPD1, both acting through indirect mechanisms of action to block SMPD1 activity. Perhexiline prevented the activation of p38 α MAPK upon stimulation with PsaDM (Fig. 10A). This suggests that SMPD1 has a role in the activation of p38 α MAPK in response to infection. However, when the inhibitor amitriptyline was used to inhibit SMPD1, there was no reduction in p38 α MAPK activation upon PsaDM stimulation (Fig. 10B). These opposite responses call into question the specificity of the inhibitors. Both are indirect inhibitors and in fact have multiple targets in the cell, as discussed in the introduction.

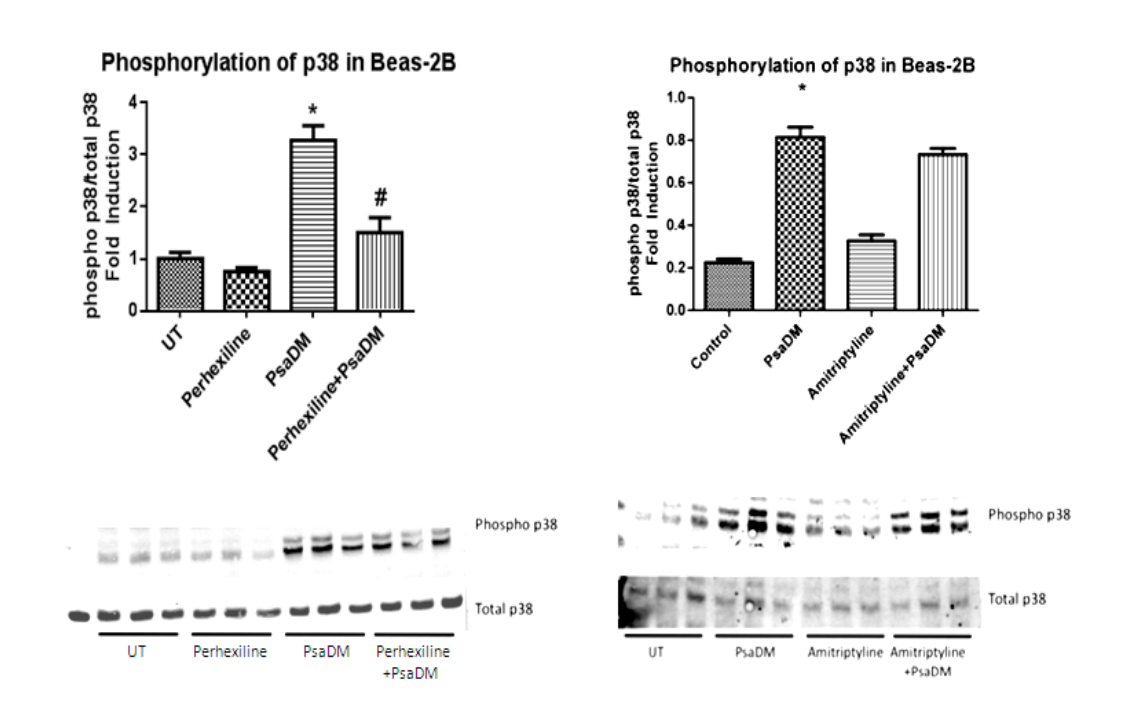


Figure 10: Phosphorylation of p38 α MAPK in the presence of SMPD1 inhibitors.

Beas-2B AECs were grown to confluency then treated with inhibitors prior to 45 min stimulation with PsaDM (heat inactivated), then cells were lysed and western blots were performed. A) treatment with perhexiline at 10 μ M for 1 hr, B) treatment with amitriptyline at 25 μ M for 1 hr (repeated 3 times). Quantification of p38 phosphorylation by fold induction. Statistical analysis 1-way ANOVA and Bonferroni correction, p < 0.05 denoted by *control v. PsaDM; # PsaDM v. Inhibitor+PsaDM.

3.3. RNA interference of SMPD1 to investigate its role in p38 α MAPK phosphorylation

3.3.1. Developing a doxycycline-inducible short hairpin RNA to decrease SMPD1 in airway epithelial cells

To gain a better grasp on this research question, I engineered AECs (BEAS-2B) expressing a short hairpin (sh)-RNA against SMPD1, which is inducible by doxycycline (Fig. 11). The sh-RNA against SMPD1

was transiently transfected in to BEAS-2B cells and the mRNA expression levels for SMPD1 were measured. The optimal amount of doxcycline to induce the knockdown of SMPD1 was 1.5μg (Fig. 11A). Then, BEAS-2B cells were then transfected to select stably transfected cells of different monoclonal populations. All of the four screened populations had significantly reduced SMPD1 mRNA expression levels (Fig. 11B). The cells from population sh-SMPD1-2 (sh2) cells were used for all subsequent experiments where sh-SMPD1 (sh) is simply depicted. By comparing the non-target (NT) cells with the SMPD1-shRNA (sh) cells, it was determined that RNA interference of SMPD1 decreased the protein level by 50% (Fig. 11C). Finally, SMPD1 activity is significantly decreased in sh-SMPD1 cells, compared to Non-Target cells using a functional enzymatic assay (Fig. 11D). Specifically, this assay measures the ability of SMPD1 to convert a sphingomyelin analogue 2-N-hexadecanoylamino-4nitrophenylphosphoryl-choline to its chromogenic metabolite, as this is indicative of SMPD1's ability to convert sphingomyelin to ceramide. The development of this inducible system allows for an overall better means to analyze the effect of SMPD1 in AECs and to analyze the role SMPD1 plays in innate immune response to bacterial infection.

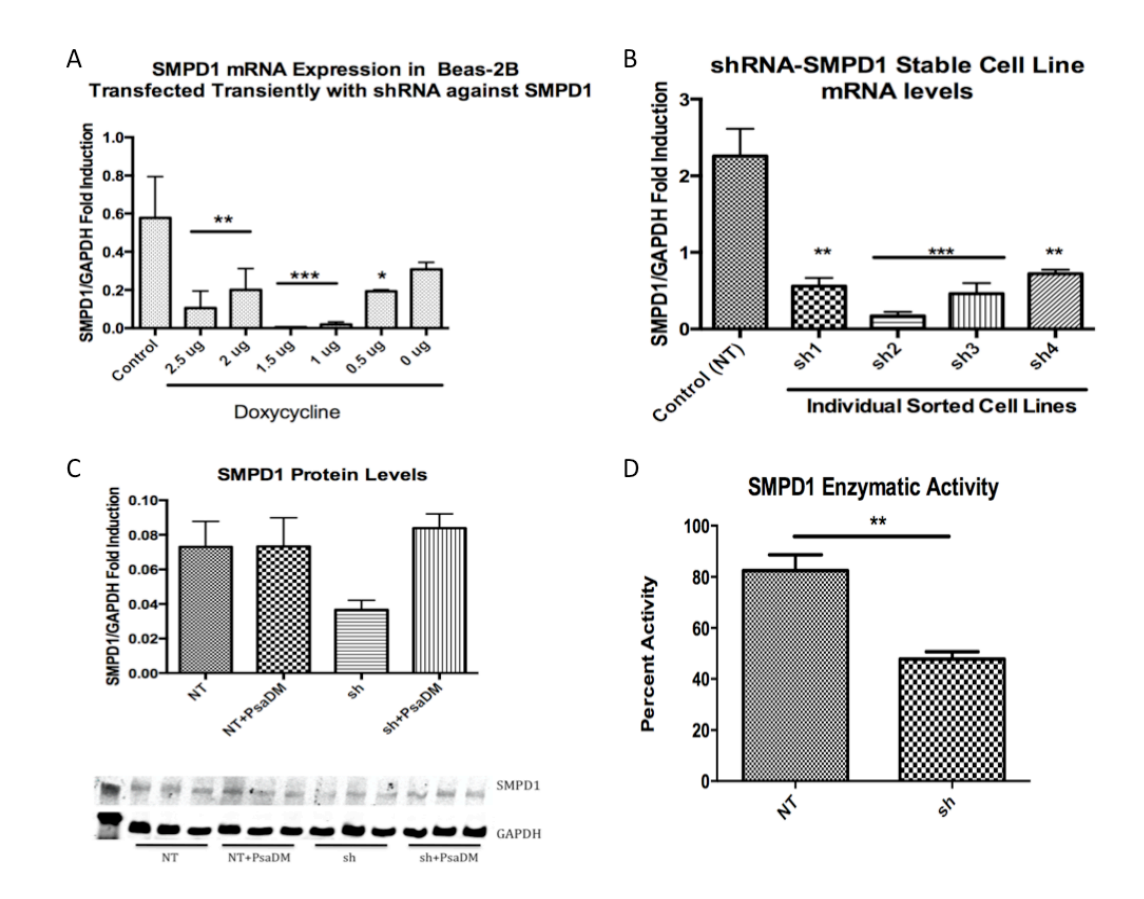


Figure 11: Creation of stable Beas-2B AECs with sh-RNA against SMPD1.

A) Transiently transfected SMPD1-shRNA constructs in Beas-2B AECs, after overnight transfection (18 hrs) and induced with 100 μ M doxycycline (repeated 3 times). Measurement of SMPD1 mRNA expression levels, where p < 0.05 denoted by * v. control. B) Stably transfected SMPD1 sh-RNA constructs in Beas-2B AECs after cell sorting and induced with 100 μ M doxycycline (repeated 3 times). Measurement of SMPD1 expression levels in 4 monoclonal cell populations, where p < 0.05 denoted by * v. control (Non-target). C) Immuno-blot to measure the protein levels of SMPD1 in the stable control (shRNA Non-target) cells and the SMPD1-shRNA cells, again induced with 100 μ M doxycycline (repeated 3 times). D) SMPD1 enzyme activity assay using 15mM 2-N-hexadecanoylamino-4-nitrophenylphosphoryl-choline, and measuring the OD at 410nm, where ** indicates p = 0.0022 (repeated 2 times).

3.3.2. AECs with SMPD1 knocked-down have dysregulated MAPKs activation

Using this novel system, p38 α MAPK phosphorylation was examined once more. In the Non-Target cells, upon stimulation with PsaDM there is an increase in p38 α MAPK phosphorylation, as expected (Fig. 12). In the sh-SMPD1 cells, there are two differences to note. First, in the untreated condition, basal phosphorylation of p38a MAPK was higher than the NON-TARGET cell (Fig. 12). Secondly, upon stimulation with PsaDM, there was no further increase in p38 α MAPK phosphorylation (Fig. 12). This would indicate that without SMPD1, there is a dysregulation in p38 α MAPK activation, which leads to the inability for p38 α MAPK signalling to mount an appropriate response in the presence of bacterial pathogens. Similar results were observed when ERK1/2 (Fig. 13) and JNK (Fig. 14) phosphorylation were examined.

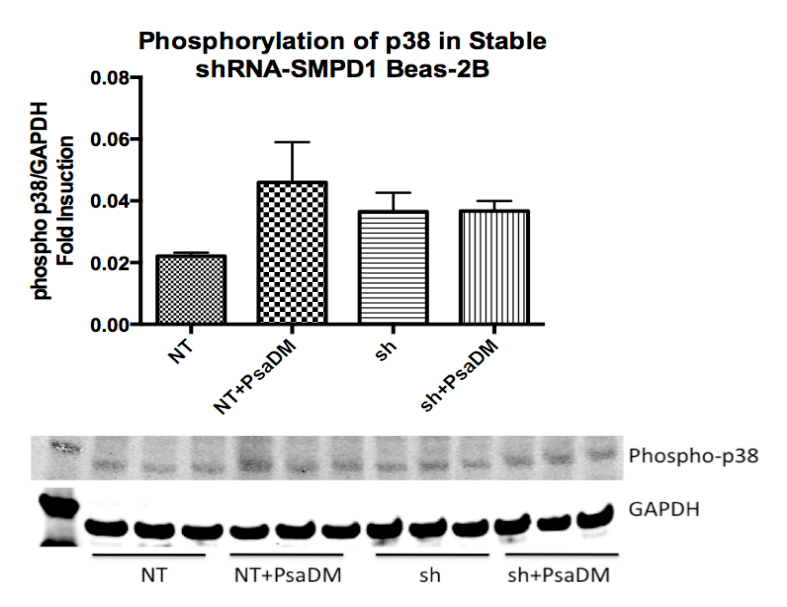


Figure 12: Phosphorylation of p38 α MAPK in stable Beas-2B AECs with sh-RNA against SMPD1.

An immuno-blot of anti-phospho-p38 α and anti-GAPDH, whereby quantification is by fold induction (repeated 3 times).

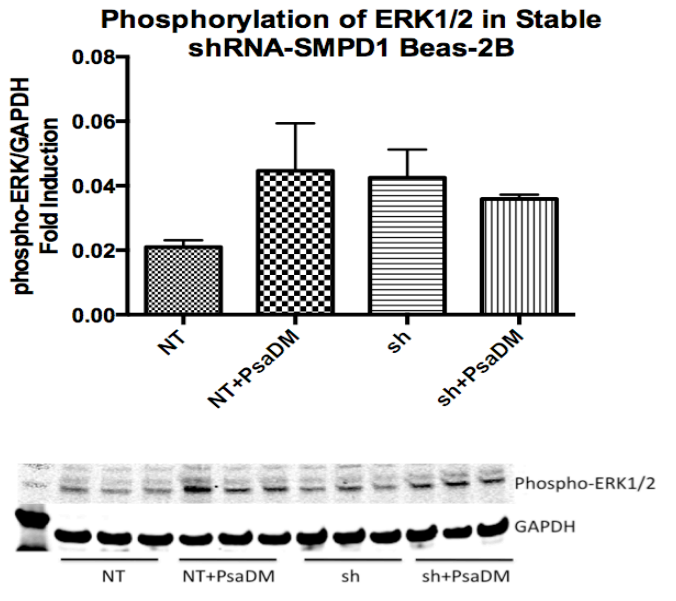


Figure 13: Phosphorylation of ERK1/ERK2 MAPK in stable Beas-2B AECs with sh-RNA against SMPD1.

An immuno-blot of anti-phospho-ERK1/2 and anti-GAPDH, whereby quantification is by fold induction (repeated 3 times).

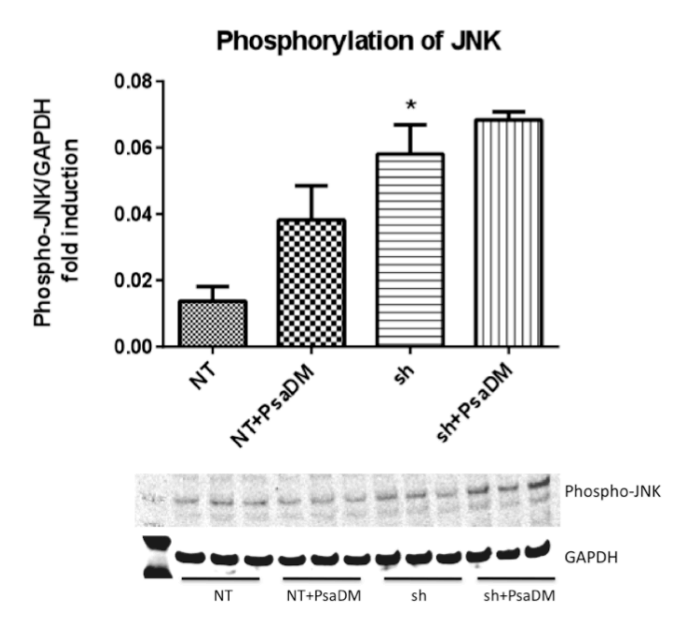


Figure 14: Phosphorylation of JNK MAPK in stable Beas-2B AECs with sh-RNA against SMPD1.

An immuno-blot of anti-phospho-JNK and anti-GAPDH, whereby quantification is by fold induction (repeated 3 times). Statistical analysis of one-way ANOVA and Bonferroni correction, where p<0.05 is denoted by * v. control.

3.3.3. p38 α MAPK activation can be rescued in sh-SMPD1 cells when transected with wild-type SMPD1

A rescue experiment was designed using the sh-SMPD1 cells and transfecting WT SMPD1 or L225P mutant SMPD1 transiently to determine the effect on p38 α MAPK phosphorylation. Transfection of WT SMPD1 into sh-SMPD1-targeted cells lowered p38a MAPK phosphyrlation in untreated condition and upon stimulation restored the increase in p38 α MAPK phosphorylation (Fig. 15A). In contrast, sh-SMPD1 cells transiently transfected with L225P mutant of SMPD1, an inactive form of SMPD1

found in NPA patients, showed a similar pattern to the non-rescued sh-SMPD1 cells (Fig. 15B). This provides further support that transfecting WT SMPD1 into sh-SMPD1 cells leads to p38 α MAPK phosphorylation levels reverting to what is seen in the Non-Target cells, both at basal level and after PsaDM stimulation.

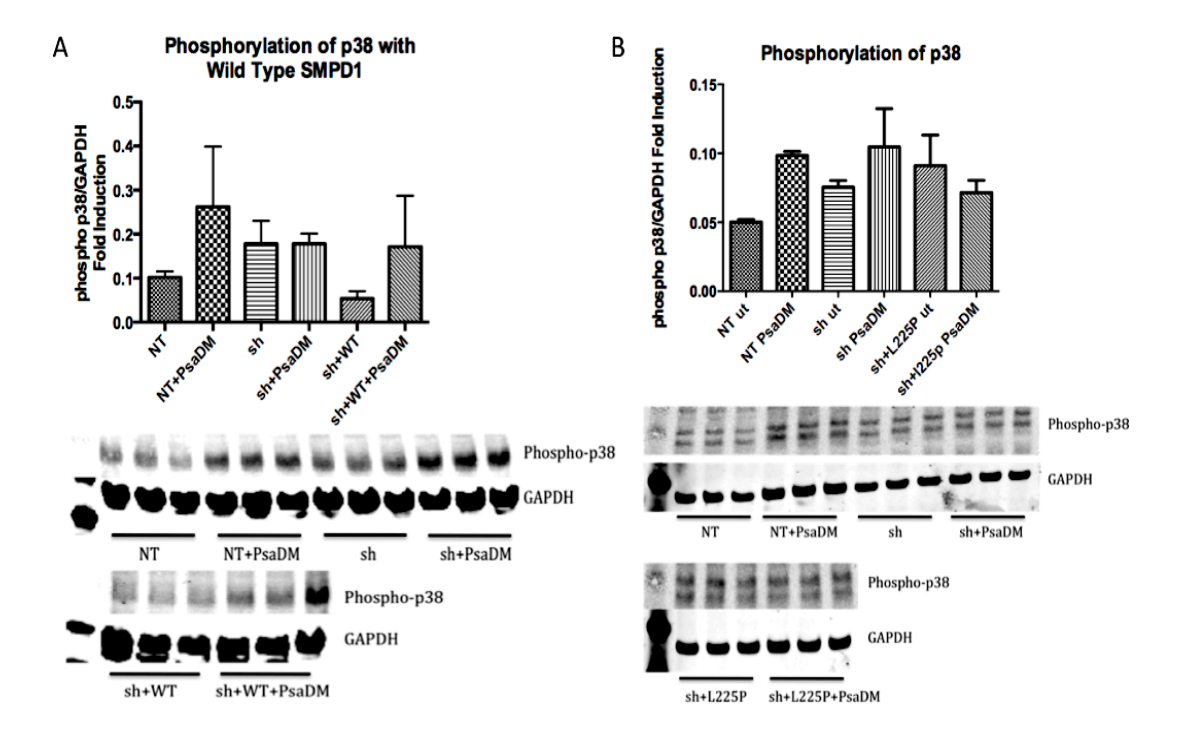


Figure 15: Rescue experiment of the phosphorylation of p38 α MAPK in stable Beas-2B AECs with sh-RNA against SMPD1. Immuno-blot of anti-phospho-p38 α and anti-GAPDH, whereby quantification is by fold induction. Transient transfections of A) WT SMPD1 and B) L225P- SMPD1 mutant, overnight, then 45 min PsaDM (heat inactivated) prior to cell lysis for immuno-blots (repeated 3 times).

3.4. NFκB Activation is lowered in AECs when transfected with an inactive form of SMPD1

As mentioned in the introduction, another important signalling pathway for innate immune responses is the activation of the transcription factor NFkB. BEAS-2B stably expressing a NFkB a luciferase reporter were transiently transfected with WT and L225P mutant of SMPD1. Upon stimulation, cells transfected with L225P mutant SMPD1 had significantly lower levels of NF κ B activation compared to the control cells stimulated with PsaDM (Fig. 16). This indicates that with non-functional SMPD1, NF κ B signalling pathway is not activated in an appropriate manner. Deregulation of this pathway has been implicated in various diseases and can result in an improper response by the host to bacterial infection.

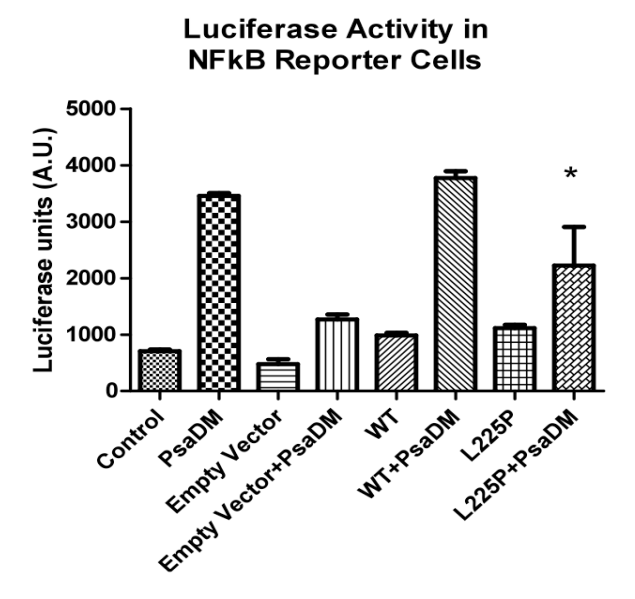


Figure 16: Measurement of NF κ B activity in Beas-2B AECs reporter cells with WT and L225P mutant SMPD1 transiently transfected.

Cells were grown to approximately 85% confluency then transiently transected overnight with either WT or L225P mutant SMPD1 constructs. Cells were deprived in minimal medium (Cnt-17) overnight, then stimulated with PsaDM (heat inactivated) for 3 hrs. Luciferase assay was used to measure levels of NF κ B activity (repeated 4 times). Statistical analysis of one-way ANOVA and Bonferroni correction, where p<0.05 is denoted by * v. control.

3.5. Elevated levels of reactive oxygen species (ROS) in sh-SMPD1 AECs

Initial experiments were performed to examine the potential role of ROS and how this may be affected by the loss of SMPD1 in BEAS-2B cells. No differences were seen however between the two groups. In order to determine if differences in ROS levels could be detected between Non-Target and sh-SMPD1 cells a FRET experiment was performed using a

ROS probe (HSP-FRET). Sh-SMPD1 cells, both untreated (ut) and treated (H₂O₂) conditions, had higher CFP/YFP ratios, meaning higher levels of ROS (Fig. 17). We next examined if there was a difference in cell survival between the Non-Target and sh-SMPD1 cells in the presence of increasing concentration of ROS. No notable differences were seen between Non-Target and sh-SMPD1 cells when exposed to hydrogen peroxide (H₂O₂) (Fig. 18).

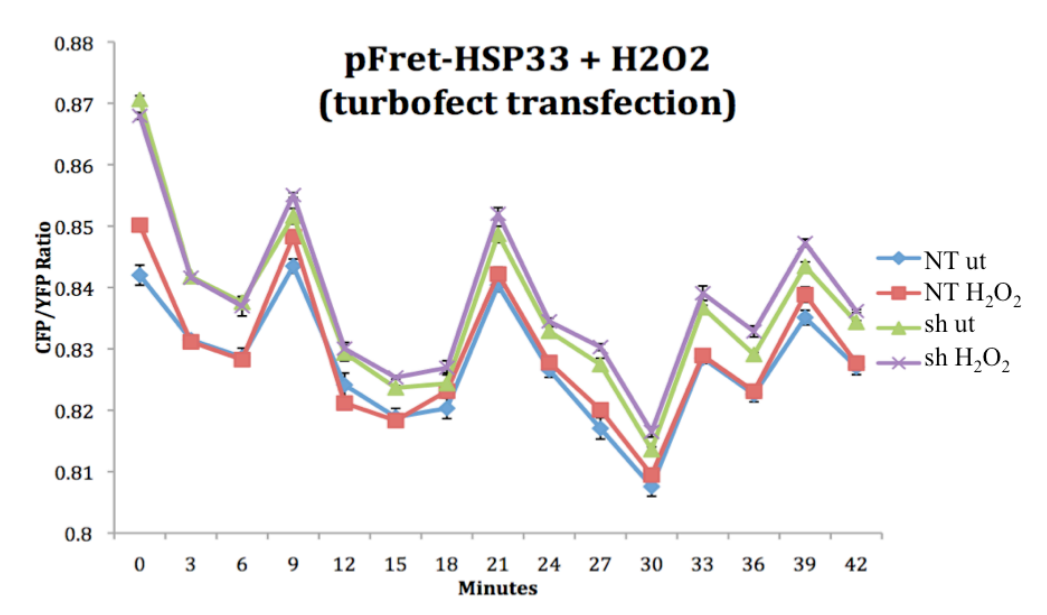


Figure 17: FRET analysis of stable Beas-2B AECs SMPD1-shRNA cell in the presence of H_2O_2 .

Using the HSP-FRET ROS probe transfected into these cells using Turbofect, HSP-FRET was excited at 430nm and fluorescence emission was obtained at 470nm using the Tecan Infinite M1000 plate reader, heated to 37°C (repeated 3 times).

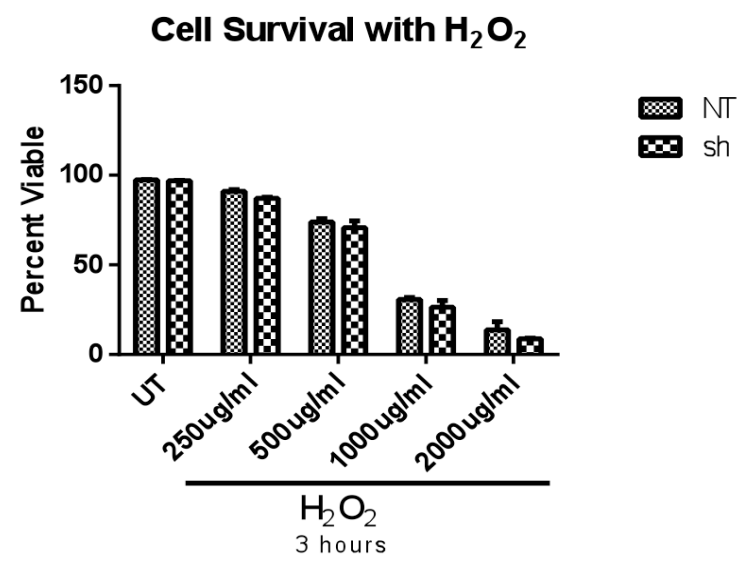


Figure 18: Cell survival in the presence of H₂O₂ as an inducer of reactive oxygen species.

Beas-2B AECs with SMPD1-shRNA knock down were grown to confluency then treated dose dependently with H₂O₂. Viable cells were counted using Trypan blue stain (repeated 3 times).

3.6. Conclusion

In this chapter, I have shown that SMPD1 is implicated in MAPK signalling in AECs, as well as NF κ B signalling. Initial results using pharmacological inhibitors of SMPD1 showed opposing responses with respect to p38 α MAPK activation (Fig. 10). This led to development of doxycycline-induced SMPD1 sh-RNA knockdown in AECs, where these cells exhibited reduced levels of SMPD1 mRNA expression, protein levels, and enzymatic activity (Fig. 11). In Figure 11C, PsaDM stimulates the protein expression of SMPD1 in the knockdown cells. This observation could be indicative of incomplete knockdown of SMPD1 or a leaky

promoter. These are important consequence of using an inducible sh-RNA knockdown system, however Non-Target sh-RNA cells are used to control for this as all comparisons with sh-SMPD1 cells are done with these Non-Target cells. When SMPD1 was knocked down there were higher basal levels of p38\alpha MAPK activation and no increase upon bacterial stimulation with PsaDM (Fig. 12). Furthermore, a similar trend was seen with ERK1/2 (Fig. 13) and JNK (Fig. 14) activation. Another aspect examined with regards to innate immune response signalling was NFκB activation. Using a luciferase assay, NFkB activation was assessed in AECs transiently transfected with wild-type and L225P-mutant SMPD1. These results showed decreased levels of NFκB activation with L225P-mutant SMPD1 (Fig. 16). Finally, reactive oxygen species are highly reactive species that are vastly involved in cellular signalling. Preliminary experiments by FRET analysis show that there are higher levels of ROS in sh-SMPD1 cells in both untreated conditions and in the presence of H₂O₂ (Fig. 17). However, there are no differences in cell survival between Non-Target and sh-SMPD1 cells exposed to H₂O₂ (Fig. 18).

Overall, the results from Chapter 3 indicate that when SMPD1 is knocked down in Beas-2B cells it causes deregulation in the innate immune system's defence against bacterial pathogens. MAPKs, in

particular p38 α , and NF κ B signalling pathways are deregulated, and levels of ROS are greater in sh-SMPD1 cells. These signalling pathways, through TLR activation, are responsible for mounting a proper immune response and when SMDP1 is knocked-down they become compromised.

of the Innate Immune System Involves Cytokine

Regulation and Consequently Neutrophil Recruitment

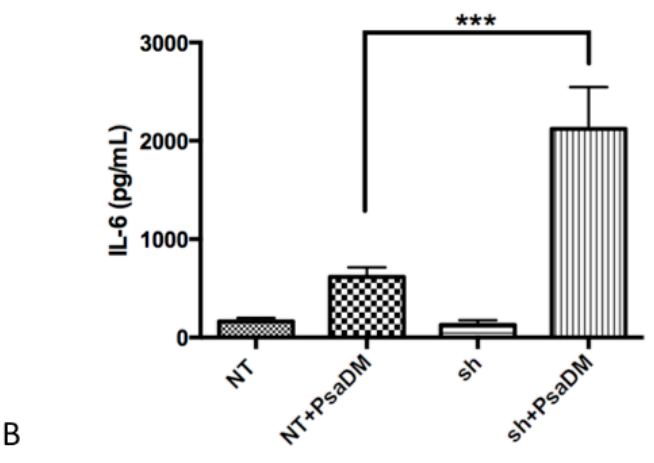
4.1. Rationale

Research in our lab has shown that CFTRΔF508 AECs have elevated levels of IL-8 in response to PsaDM¹06. Additionally, due to the hyperactivation of p38α and ERK1/2 MAPKs mentioned previously, higher levels of IL-6 mRNA expression have been demonstrated in CFTRΔF508 AECs challenged with PsaDM88. This increases neutrophil recruitment. Moreover, there is a necessary threshold of p38α MAPK activation in order to trigger neutrophil recruitment⁶⁹. Looking along the same lines, the Non-Target and sh-SMPD1 cells were used to examine how cytokines and neutrophil recruitment was affected by the loss of SMPD1 activity.

- 4.2. Airway epithelial cells lacking SMPD1 exhibit hypersecretion and increased expression levels of cytokines
- 4.2.1 Higher concentrations of IL-6 and IL-8 are secreted from AECs with SMPD1 knocked-down when challenged with PsaDM

IL-6 and IL-8 are two of the major cytokines secreted in response to activation of airway epithelial cells resulting in increased neutrophil recruitment¹⁰⁷. Therefore their levels secreted into the supernatant were measured. When AECs are stimulated with PsaDM the levels of both IL-6 (Fig. 19A) and IL-8 (Fig. 19B) are significantly increased in the sh-SMPD1 cells compared to Non-Target cells. This corresponds with the higher overall levels of MAPK phosphorylation shown in Chapter 3.

A
IL-6 Levels in Beas-2B with Stable SMPD1 Knockdown



IL-8 Levels in Beas-2B with Stable SMPD1 Knockdown

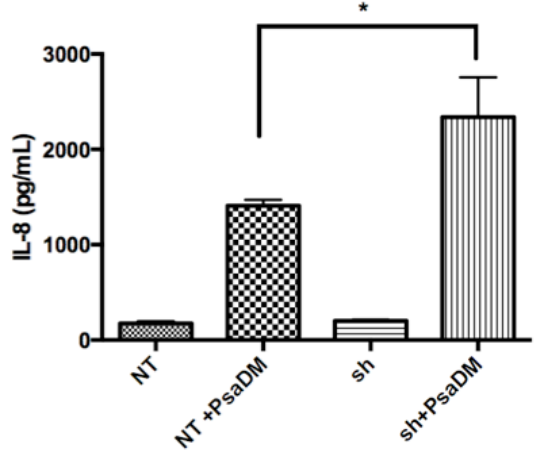


Figure 19: Measurement of secreted IL-6 and IL-8 by ELISA in stable Beas-2B AECs SMPD1-shRNA cells.

Cells were grown to confluency then stimulated with PsaDM (heat inactivated) for 6 hrs. Supernatants were collected and used to measure secreted cytokine levels by ELISA (repeated 3 times). Statistical analysis of one-way ANOVA and Bonferroni correction, where p<0.05 is denoted by *.

4.2.2 An overall increase in cytokine expression exists in sh-SMPD1 AECs

To determine whether this increased expression was specific to IL-

6 and IL-8, the expression levels of ten cytokines and chemokines were

investigated (Table 5). Non-Target and sh-SMPD1 AECs were exposed to PsaDM for 0, 1h, 3h, 6h and 18h and the mRNA expression levels of cytokines involved in the innate immune response to bacterial infection and inflammation measured at every time point tested. IL-8 mRNA levels were significantly higher in the sh-SMPD1 cells than the NON-TARGET cells (Fig. 20A). IL-6 had a trend to higher levels at the 3h but the difference was not significant (Fig. 20B). CCL20 levels were significantly increased in sh-SMPD1 cells at 3 hrs and 6 hrs of PsaDM stimulation (Figure 20C). The mRNA expression levels for RANTES are significantly increased in sh-SMPD1 cells at time zero, 3 hrs, 6 hrs, and 18 hrs of challenge by PsaDM (Fig. 20D). CCL13 was also significantly increased at all time points from 1 hr to overnight in sh-SMPD1 cells (Figure 20E). The expression levels in sh-SMPD1 cells of CXCL12 were significantly increased in the early time points of zero to 3 hrs (Fig. 20F). The mRNA levels of eotaxin-1 were significantly higher in sh-SMPD1 cells at the 6 hr and 18 hr time points (Fig. 20G). GM-CSF had significantly more mRNA levels in sh-SMPD1 cells compared to Non-Target cells at 3 hrs of PsaDM stimulation (Fig. 20H). CCL-1 had significantly higher levels in the sh-SMPD1 cells at the time points of 3 hrs and 18 hrs (Fig. 201). Finally, the last cytokine analyzed in this panel, was $Gro-\alpha$, which had significantly

elevated expression levels in sh-SMPD1 cells from 3 hrs onwards (Fig. 20J). The overarching message is that upon stimulation of cells with PsaDM, the sh-SMPD1 cells in general have significantly higher levels of cytokines involved in the innate immune response and inflammation.

Table 5: Brief Description Cytokines Analyzed

Cytokine	Description
IL-8	a strong chemotractant for neutrophils
IL-6	involved in acute phase of immune response
CCL20	involved in chemotaxis of leukocytes
Rantes	involved in the recruitment of leukocytes to the site of inflammation
CCL13	implicated more in allergy
CXCL12	a strong chemotractant for lymphocytes
Eotaxin-1	selectively recruits eosinophils to the site of inflammation
GM-CSF	a white blood cell growth factor
CCL1	a glycoprotein with a role in inflammation and immuno-regulation,
Gro-α	important in inflammation and neutrophil recruitment

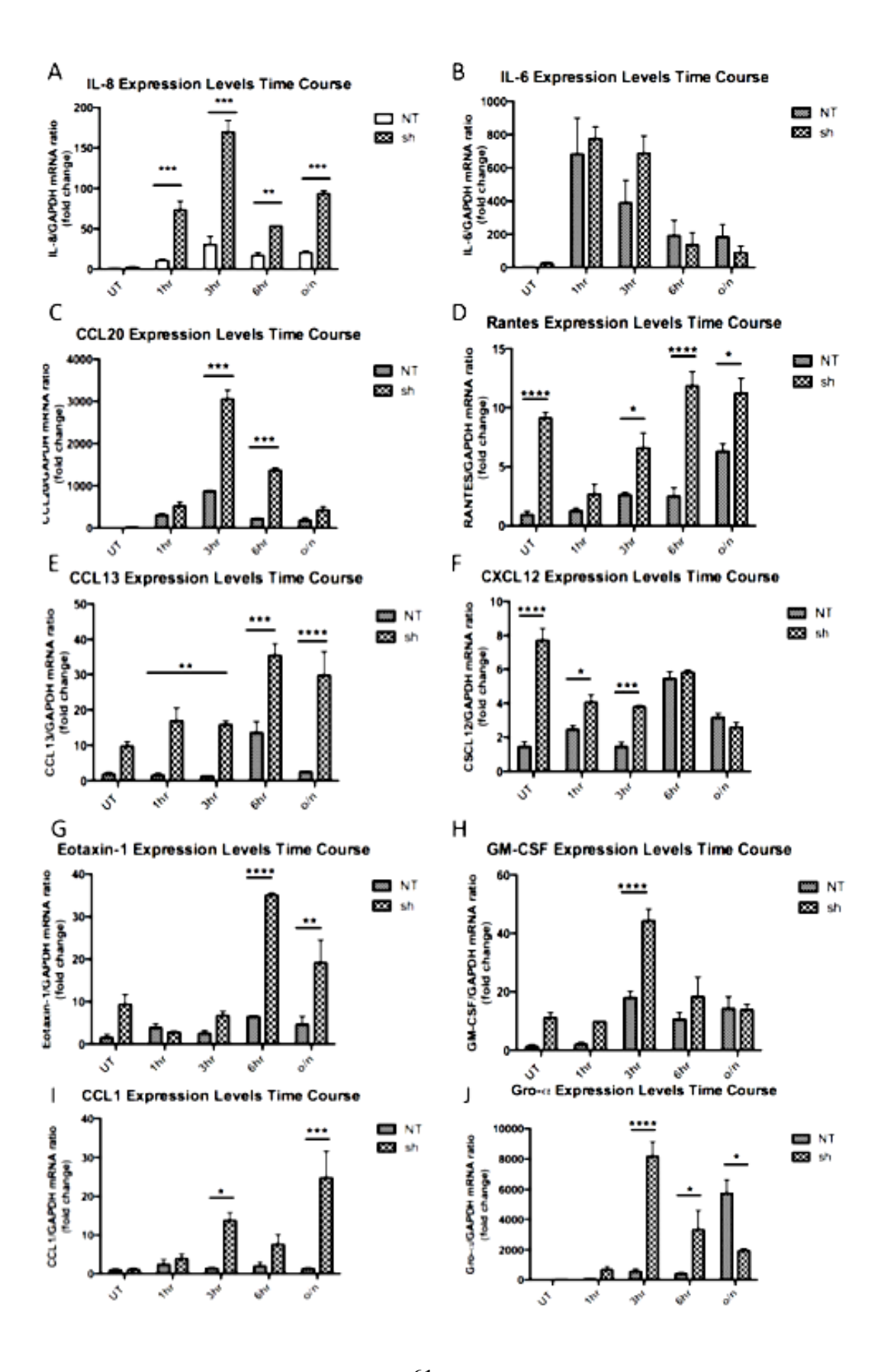


Figure 20: Time course of mRNA expression levels of various cytokines upon 3 hr PsaDM stimulation in stable Beas-2B AECs SMPD1-shRNA cells.

Cells were grown to confluency then stimulated with PsaDM (heat inactivated) for 3 hrs. mRNA was extracted and expression levels of cytokines were measured by qPCR (repeated 3 times). Statistical analysis of one-way ANOVA and Bonferroni correction, where p<0.05 is denoted by *.

4.2.3. Caspase-1 dependent cytokines also elevated in sh-SMPD1 AECs

Additionally, IL-1 β and IL-18, important inflammatory mediators, were examined. Both these cytokines are capsase-1 dependent. Caspase-1 is an important enzyme in inflammation and regulation of cell death, where it activates certain molecules, such as IL-1 β and IL-18^{108,109}. IL-1 β mRNA levels are significantly increased in sh-SMPD1 cells upon PsaDM stimulation (Fig. 21). IL-18 mRNA levels are also significantly higher in sh-SMPD1 cells at basal level (Fig. 21). Upon stimulation with PsaDM, sh-SMPD1 cells have higher expression levels of IL-18; however this did not reach statistical significance (Fig. 21). This data corresponds well with what was initially seen in Figure 20, whereby an overall increase in cytokine expression levels were seen in the cells with shRNA against SMPD1.

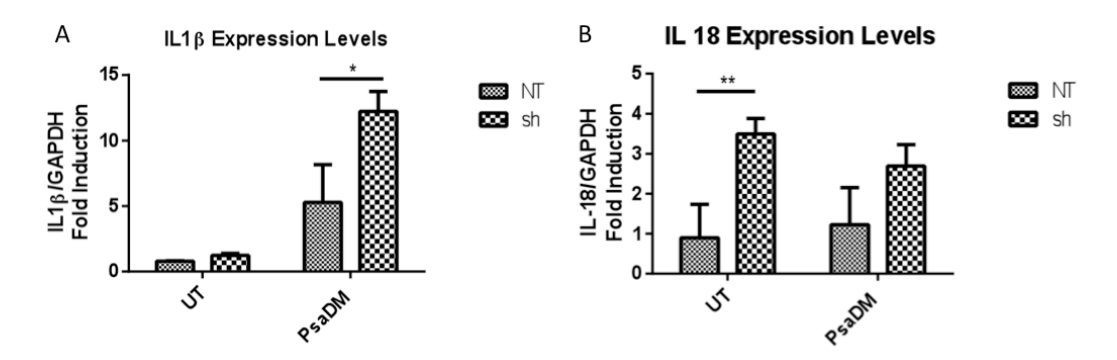


Figure 21: Expression levels of caspase-1 dependent cytokines.

qPCR analysis was done to examine the levels of mRNA expression for A) IL-1 β and B) IL-18 (repeated 3 times). Statistical analysis of one-way ANOVA and Bonferroni correction, where p<0.05 is denoted by *.

4.3. A consequence of elevated cytokine levels in sh-SMPD1 AECs is the recruitment of more neutrophils

Neutrophils play an important role in innate immunity. They are seen as the first line of defence against invading pathogens. PsaDM stimulates significant neutrophil recruitment in both Non-Target and sh-SMPD1 cells (Fig. 22). Furthermore, there are significantly more neutrophils recruited at the basal level in sh-SMPD1 cells compared to Non-Target cells, as well as a significantly higher number of neutrophils recruited in sh-SMPD1 cells when challenged with PsaDM compared to NON-TARGET cells challenged with PsaDM (Fig. 22). This data corresponds with the significantly increased levels of IL-8 in sh-SMPD1 cells upon PsaDM stimulation as seen in Figure 20A.

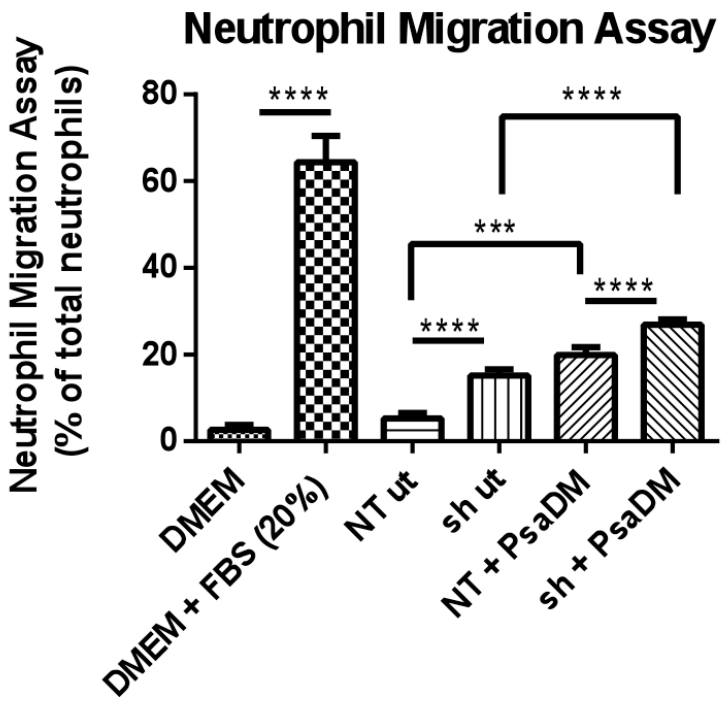


Figure 22: Neutrophil recruitment assay.

Conditioned medium, from 3 hr PsaDM (heat inactivated) stimulation with Beas-2B SMPD1-shRNA cells, was used to stimulate neutrophil recruitment (repeated 3 times). Statistical analysis of one-way ANOVA and Bonferroni correction, where p<0.05 is denoted by *.

4.4 Conclusion

In this chapter, I have shown that AECs that have SMPD1 knocked-down have significantly increased cytokine production and subsequently recruit more neutrophils. In the cytokine profile for mRNA expression levels, all ten cytokines demonstrated higher levels of expression at one time point or another (Fig. 20). Additionally, IL-6 and IL-8 were secreted at higher levels upond stimulation with PsaDM in the sh-SMPD1 cells (Fig. 19). Also, sh-SMPD1 cells had higher levels of IL-1β and IL-18, capase-1

dependent cytokines, that are involved in inflammation and cell death regulation (Fig. 21). Finally, more neutrophils were recruited by cells lacking SMPD1 in the untreated condition as well as upon bacterial stimulation by PsaDM (Fig. 22).

The results from this chapter suggest that SMPD1 has a role in regulation of cytokine production in AECs. Overall, increased expression of cytokines and more IL-6 and IL-8 secreted by sh-SMPD1 cells leads to a higher number of neutrophils being recruited. This coincides with the increase in MAPKs phosphorylation seen in Chapter 3.

CHAPTER 5: Disruption of Intracellular Localization and Protein-Protein Interactions of the SMPD1 (L225P)-disease causing-mutant

5.1. Rationale

Translocation of SMPD1, from the lysosome to the outer leaflet of the membrane, is essential to its functioning. Therefore it was important to examine if this process was affected by the SMPD1 (L225P)-disease causing-mutant and whether this may give a clue to the increased cytokine expression described in the previous chapter. This was done by immunofluorescence to visualize GFP-tagged SMPD1, and by Tandem Affinity Purification, to identify possible binding partners that are involved and /or required for this process.

5.2 SMPD1 (L225P)-disease causing-mutant shows impaired translocation to outer-leaflet of cell membrane by immunofluorescence

A new system was developed to be able to easily visualize SMPD1 by tagging the protein with GFP. Using the Hek-Flp-IN system described in the Methods section, WT SMPD1 cells and L225P mutant SMPD1 cells were created in HEK293 cells background. When doxycycline was given to induce SMPD1 expression, a large increase GFP (green) was observed

(Fig. 23). Hoechst was used to stain the DNA (blue), and actin is stained phalloidine (red) (Fig. 23). This shows that this system is a good on/off switch of SMPD1 by doxycycline. Furthermore, supplementary material in the Appendix, demonstrates that presences of doxycycline induces the mRNA expression of SMPD1 in this system (Fig. 25A), and that when doxycycline is washed out it reverts SMPD1 expression back to basal levels (Fig. 25B). WT SMPD1 in the presence of doxycycline with PsaDM seems to have green punctates at the cell membrane, which is indicative of SMPD1's translocation to the cellular membrane upon bacterial stimulation (Fig. 23A, arrows). In contrast, with the L225P mutant SMPD1 in the presence of doxycycline with PsaDM, there seems to be a lack of distinct punctuates at the cell membrane (Fig. 23B, arrows).

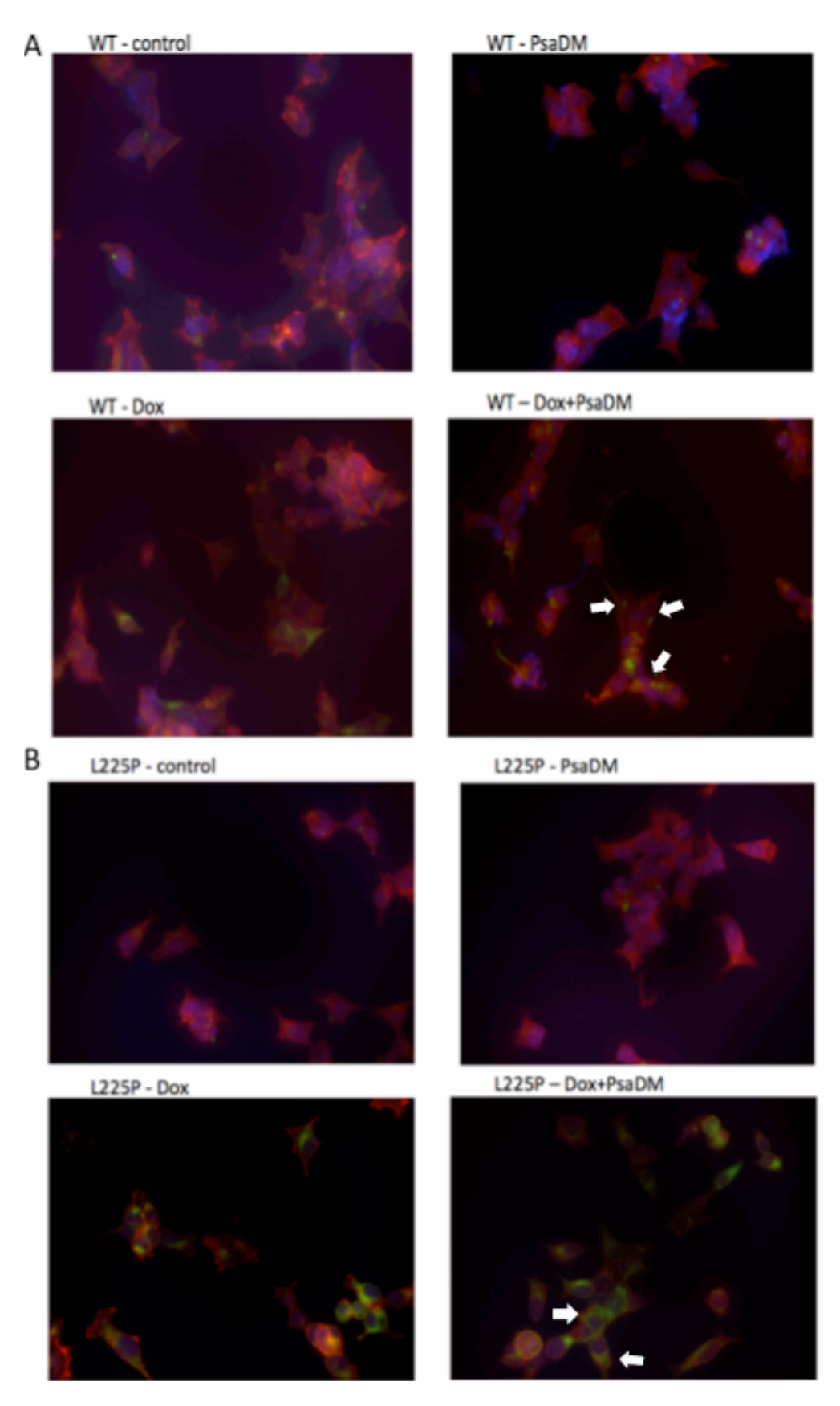


Figure 23: Immunofluorescence in Hek-Flp-IN cells expressing WT or L225P mutant SMPD1.

Hek-Flp-IN WT and L225P cells were plated and treated with $100\mu M$ doxycycline and 30 min PsaDM (heat inactivated) stimulation. Slides were visualized at 200X magnification through Olympus BX51 filters, using Image Pro 7 software to obtain images. SMPD1 is GFP tagged, Alexa568 Phalloidine used for actin and Hoescht for DNA staining (repeated 2 times).

5.3.Identification of potential novel binding partners of SMPD1 using tandem affinity purification followed by mass spectrometry analysis

In order to determine whether the presence of the L225P mutation changed protein-protein interactions, tandem affinity purification was performed using the cell system described in section 5.2. Four conditions were examined: WT SMPD1 untreated, WT SMPD1 stimulated with PsaDM, L225P mutant SMPD1 untreated, and L225P mutant SMPD1 stimulated with PsaDM. The results from the purification are illustrated in Fig. 24.

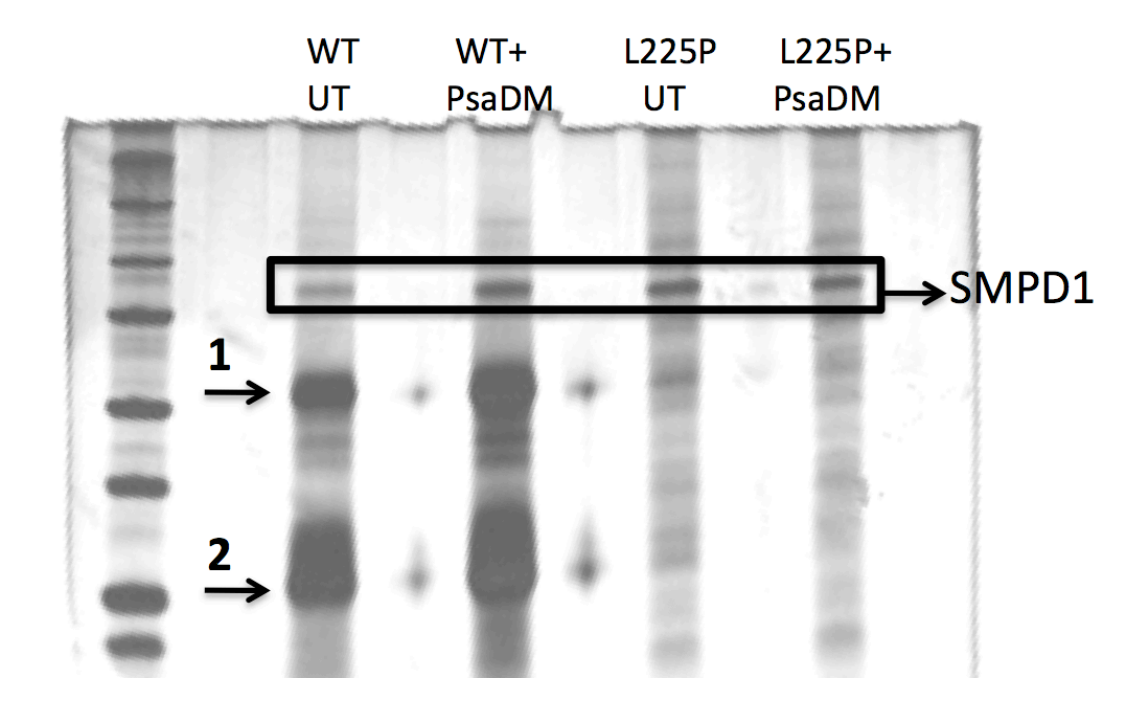


Figure 24: TAP SDS-PAGE gel.

Hek-Flp-IN cells (TAP tagged) were induced by 500ng/mL of doxycycline and grown to confluency, then stimulated with PsaDM (heat inactivated) for 1 hr. Samples were loaded on to gel after following the TAP protocol. Bands were visualized by silver staining and subsequently cut out, indicated by the arrows, for mass spectrometry analysis.

Bands were visualized by silver staining, and those bands that were different between the WT and L225P mutant (indicated by arrows) were cut out and sent for analysis by mass spectrometry. Data collected was initially analyzed from the mass spectrometry using Scaffold Viewer. This program allows one to view the protein hits as a list, or in Venn diagrams, (Appendix, Fig. 26). In order to specifically identify protein as possible binding partners with SMPD1, the online analysis tool, PANTHER Classification System 9.0 was used. Table 5 summarizes the top hits for

each band isolated from the TAP experiment. The numbers in the last four columns represent spectral counts, which are accepted semi-quantitative method to measure protein abundance in proteomic studies such as this. Band 1 has been assigned as Vimentin, an intermediate filament protein and therefore important to maintain the integrity of the cell and resists stress¹¹⁰. With respect to the spectral counts there is a high possibility that this protein does interact with SMPD1 WT but not L225P mutant. Band 2, which is also present in the WT conditions and not the mutant, has been assigned to ribosomal protein S3 (RPS3), as it has much higher spectral counts, and interestingly the number of spectral counts increases upon stimulation with PsaDM (Table 5).

		Molecular	WT	WT	WT	WT
Identified Proteins	Accession Number	Weight	ut2	psadm2	ut3	psadm3
	gi 1090507					
ATP synthase:SUBUNIT=alpha	(+20)	60 kDa	5	4		
60 kDa SS-A/Ro ribonucleoprotein isoform 1	~:!10070C0FC					
ribonucleoprotein isoform 1 [Homo sapiens]	gi 108796056 (+17)	59 kDa	7	10		
polypyrimidine tract binding	(127)	33 KBG	<u> </u>	10		
protein 1, isoform CRA_a [Homo	gi 119581556					
sapiens]	(+21)	59 kDa	2	2		
chaperonin containing TCP1,	-:1110620145					
subunit 7 (eta), isoform CRA_b [Homo sapiens]	gi 119620145 (+16)	59 kDa	2	1		
chaperonin containing TCP1,	(+10)	JJ KDU				
subunit 4 (delta), isoform CRA_c	gi 119620392					
[Homo sapiens]	(+12)	58 kDa	2	1		
Chaperonin containing TCP1,	gi 109730511	F7.15	_			
subunit 2 (beta) [Homo sapiens] aspartyl-tRNA synthetase,	(+13) gi 119632022	57 kDa	5	4		
isoform CRA_a [Homo sapiens]	gi 119632022 (+14)	57 kDa	5	3		
PRP19/PSO4 pre-mRNA	(111)	37 KDU	-			
processing factor 19						
homolog (S. cerevisiae),						
isoform CRA_b [Homo sapiens]	gi 119594311 (+6)	55 kDa	1	2		
vimentin, isoform CRA_a	gi 119606621	33 KDa	-			
[Homo sapiens]	(+18)	54 kDa	41	17		
heterogeneous nuclear						
ribonucleoprotein K, isoform	gi 119583079					
CRA_a [Homo sapiens]	(+26)	51 kDa	5	3		
Tubulin, beta 2C [Homo sapiens]	gi 12803879 (+13)	50 kDa	1	5		
heterogeneous nuclear	(+13)	JU KDa		<u> </u>		
ribonucleoprotein H1 (H),	gi 119574192					
isoform CRA_a [Homo sapiens]	(+13)	49 kDa	10	6		
SERPINE1 mRNA binding protein	gi 12803339	4415	_	_		
1 [Homo sapiens] solute carrier family 25	(+11)	44 kDa	7	6		
solute carrier family 25 (mitochondrial carrier; adenine						
nucleotide translocator),						
member 5, isoform CRA_c	gi 119610276					
[Homo sapiens]	(+3)	33 kDa			4	7
ribosomal protein L7a, isoform CRA_a [Homo sapiens]	gi 119608467	22 1/02			6	7
CRA_a [Horno sapiens]	(+24) gi 119609105	33 kDa			0	/
prohibitin 2 [Homo sapiens]	(+8)	32 kDa			2	15
ribosomal protein S2, isoform	gi 119605998					
CRA_a [Homo sapiens]	(+31)	31 kDa	1		3	3
hCG33299, isoform CRA_a [Homo sapiens]	gi 119597983 (+24)	30 kDa			6	11
ribosomal protein L7, isoform	gi 119607405	JU KDa			U	11
CRA a [Homo sapiens]	(+16)	30 kDa			2	5
ribosomal protein S6, isoform	gi 119579045					
CRA_e [Homo sapiens]	(+16)	29 kDa			7	9
ribosomal protein L8, isoform	gi 119602454	20 1/5-				
CRA_b [Homo sapiens] ribosomal protein S3 [Homo	(+15) gi 119595369	28 kDa			2	1
sapiens]	(+17)	27 kDa			12	22
ribosomal protein S8, isoform	gi 119627428		1		1	
CRA_a [Homo sapiens]	(+10)	27 kDa			6	1
ribosomal protein L13, isoform	gi 119587128	24 5			1.	_
CRA_a [Homo sapiens]	(+20) gi 119575919	24 kDa			4	5
histone 1, H1c [Homo sapiens]	gi 1195/5919 (+28)	21 kDa			1	2
בייסייסן	72	_ LI NDa	1	<u> </u>		-

Table 6: Top hits identified from mass spectrometry analysis using PANTHER Classification System 9.0.

This table summarizes the top hits from the mass spectrometry analysis. The bolded proteins are of further interest to examine their role and potential interaction with SMPD1.

5.4. Conclusions

In Chapter 5 the localization and potential binding partners of SMPD1 were explored. In terms of localization, a method for visualization by immunofluorescence was developed. SMPD1, both wild-type and L225P mutant, are GFP labeled and the preliminary data show that there is a possible inability of SMPD1 translocation to the cell membrane in the L225P mutant cells, as seen by a lack of punctate formation upon stimulation by PsaDM (Fig. 23). The TAP and mass spectrometry analysis revealed two interesting binding partners from the two bands that were present in the WT but not in the L225P mutant samples (Fig. 24). However, both hits, vimentin and RPS3, need to be validated to determine the extent of interaction between these proteins and SMPD1.

This final chapter in my thesis provides interesting data regarding the translocation process of SMPD1 and interactions it may have with other proteins. Further studies are required, but from these results it seems as though the SMPD1 (L225P)-disease causing-mutant lacks the ability to reach the cell membrane in order to initiate the conversion of sphingomyelin to ceramide.

Chapter 6: Conclusions and Future Directions

6.1. Summary of Results and General Discussion

6.1.1. SMPD1 is required for the appropriate activation of MAPKs in AECs to trigger the necessary immune response when faced with bacterial challenge

MAPK signalling is a necessary pathway involved in the immune system's response to pathogens. p38α, ERK1/2, and JNK MAPKs are activated to certain degrees, depending on the response that is necessary. When SMPD1 is knocked-down in AECs, it affects the response of all three of these protein kinases. The cells lacking or exhibiting reduced SMPD1 activity exhibit higher basal levels of phosphorylated p38α, ERK1/2, and JNK MAPKs (Figures 12-14). Furthermore, upon stimulation with PsaDM, these cells did not have increased phosphorylation, as was seen with Non-Target cells. In terms of activation of p38 α MAPK, when sh-SMPD1 cells were transfected with WT SMPD1, the levels of phosphorylated p38 α MAPK, both basal and stimulated, reverted back to those of the Non-Target cells (Figure 15A). This means that SMPD1 is directly involved in preserving proper activation of MAPKs in AECs.

6.1.2. AECs lacking SMPD1 demonstrated an over-production of various cytokines implicated in inflammation and significantly more neutrophils recruited

Higher expression levels of numerous pro-inflammatory cytokines in sh-SMPD1 cells, both at basal levels and upon stimulation via bacterial products were also seen (Figure 20). For certain cytokines, like RANTES and CXCL12, there was significantly more mRNA in sh-SMPD1 cells. In general, upon stimulation with PsaDM, all the cytokines examined tended to have higher expression levels in sh-SMPD1 cells at certain time points over 18 hrs, but mostly at 3 hrs of stimulation. In addition to increased production and secretion of cytokines, it is not surprising that neutrophil levels in these cells were also increased significantly (Figure 22). This increase was also seen at the basal level and after 3 hr challenge with PsaDM. Clearly for IL-8 changes in mRNA expression reflects changes in protein function as higher levels of neutrophils were seen. However, with respect to the other cytokines examined in Figure 20, further analysis is necessary in order to determine if changes in cytokine mRNA expression reflect changes in protein function. For example, CXCL12 mRNA levels were increased in sh-SMPD1 cells and to examine if this is reflected in increased protein function, the recruitment of lymphocytes can be examined.

Furthermore, caspase-1 dependent cytokines were also elevated. IL-1β, a proinflammatory cytokine, exhibited increased levels upon bacterial challenge which is seen in the Non-Target cells' response, and is an expected response to bacterial pathogens. However, the sh-SMPD1 cells showed significantly higher levels than the Non-Target cells upon PsaDM stimulation, which could lead to hyper-inflammation (Fig. 21A). Additionally, IL-18, which is related to severe inflammation, showed higher basal levels in the sh-SMPD1 cells can also lead to hyper-inflammation (Fig. 21B).

6.1.3. Impaired translocation of SMPD1 (L225P)-disease causing-mutant to the outer-leaflet of the cell membrane upon bacterial stimulation

With regards to translocation of SMPD1, an inducible system that facilitates visualization of GFP-tagged SMPD1 by IF was generated (Figure 23). This system works well, but requires additional optimization, in order to be able to obtain valuable data from this method. Quantitatively data was unable to be obtained; however, qualitatively, the images obtained show that the cells with the L225P mutant is unable to form punctates at the surface of the cell membrane, while the wild-type cells clearly form these punctates (Fig. 23). Image analysis or automated

quantitative analysis methods can be applied to this system in order to obtain subcelllular quantification of the localization of SMPD1.

6.1.4. Potential novel protein interactions of SMPD1

Finally, a method was developed to examine potential binding partners of SMPD1 through tandem affinity purification followed by mass spectrometry analysis (Table 6). This experiment generated several interesting hits, which need to be further explored. Given that the translocation of SMPD1 from the lysosome to the cell membrane is essential for this enzyme to facilitate the production of ceramide from sphingomyelin, an interaction vimentin is plausible. Vimentin is a protein involved in maintaining cell shape, adhesion and preserves the integrity of the cytoskeleton. Specifically, it has a role in supporting and anchoring organelles to the cell membrane¹¹¹.

Moreover, the other potential protein interaction identified was with RPS 3. This protein is especially interesting as it has been shown to be implicated in mitosis as a mictotubule-associated protein 112 , linked to ROS and mitochondrial DNA damage 113 , and more notably, interacting with bacterial pathogens 114 , as well as interacting with NF κ B $^{115-117}$. An alternative hypothesis involving SMPD1's role in innate immunity, given that RPS3 is important to activation of NF κ B regulated genes and SMPD1

and RPS3 potentially interact, is that SMPD1's involvement in regulation of innate immunity is via signalling through NF κ B pathway by interacting with RPS3.

The other proteins highlighted (Table 6) are Pre-mRNA processing factor 19 (PRP19) and Histone 1 (H1c). Band 1 (Fig. 24) could also potentially be assigned to PRP19, which has a role in mediating DNA damage responses in cells. It has been shown that loss of this protein has induced apoptosis and decreased cell survival¹¹⁸. Lack of this band in the mutant conditions would lead to the hypothesis that SMPD1 is involved in apoptotic signalling via interaction with PRP19; however, it is important to note that this protein had very few spectral counts in the analysis. The lower band, Band 2 (Fig. 24), which is also present in the WT conditions and not the mutant, may alternatively be assigned as Histone 1 (H1c). H1c is implicated in apoptosis with respect to regulation of apoptosme formation¹¹⁹. However, like PRP19, H1c has a low spectral count (Table 6). To fully interpret these results, validation of these top hits must be done to determine if in fact these proteins interact with SMPD1, which can be done by co-immunoprecipitation.

6.2. Conclusions

Taken together, these results imply a critical role for SMPD1 in attenuating the immune response. In diseases such as CF and NPD, a decrease in SMPD1 leads to the accumulation of precursors to MAKPs signalling resulting in impaired immune response upon bacterial challenge. In the literature, the effects of SMPD1 on MAPK pathways are not well understood. One group saw no difference in p38 α MAPK activation upon bacterial stimulation in human fibroblasts⁹⁴, while another group saw lower p38\alpha MAPK activation in HeLa cells95. Both of these outcomes differ from what was seen in our system using sh-SMPD1-RNA against SMPD1 where basal levels of p38 α MAPK were elevated. With regards to cytokine levels, in SMPD1 KO mice there was significantly higher release of cytokines in response to P. aeruginosa²³, and this coincides well with what was seen in Figure 20 in the sh-SMPD1 cells. However, it has also been shown that IL-6 levels are decreased in the presence of SMPD1 inhibitors99. Based on our data with SMPD1 inhibitors, it is clear that interpreting results with inhibitors should be done carefully, as they may not necessarily be as selective as thought and the extent of off target effects may not necessarily be well understood. Furthermore, it is quite clear from our research and the literature, that the response to challenge by *P. aeruginosa* is context dependent and cell-type specific.

Based on the results of this thesis involving potential binding partners, if the SMPD1 (L225P)-disease causing-mutant cells lack this interaction with vimentin, it would account for the lack of punctates seen (Fig. 23), and thus the inability for SMPD1 to reach the outer-leaflet of the cell membrane to produce ceramide. Furthermore, based on roles of RPS 3 and the pathways it is involved in, lacking an interaction with RPS 3 in the SMPD1 (L225P)-disease causing-mutant cells, would result in a dysfunctional immune response to bacterial challenge, as seen throughout Chapters 3 and 4, with respect to MAPKs activation, cytokine production, and neutrophil recruitment. The significance of these results relates directly to the clinical phenotype of NPD patients, in that they have increased susceptibility to respiratory infections, which is the major cause for death in these patients.

In conclusion, the results suggest that SMPD1 affects the balance of sphingolipids, which is essential to signalling pathways necessary for AECs to combat bacterial pathogens. The data shows that when SMPD1 is knocked down, there is an elevation of MAPK activation, an overall elevation of cytokines produced, and greater number of neutrophils

recruited. Alternatively, SMPD1 can be viewed as a negative regulator of cytokines. The next step is to elucidate the mechanisms by which this is occurring, in order to specifically determine how SMPD1 is involved and how a lack of or non-functional SMPD1 leads to deregulation of signalling pathways involved in innate immunity. Therefore, understanding the role played by SMPD1 in host defense mechanisms of the lungs is crucial to develop novel therapies aimed at improving the quality of life of patients suffering from CF and NPD.

6.3. Future Directions

Additional work is required in order to understand the mechanism by which SMPD1 is exerting its affects as seen in our results. The NFκB pathway was deregulated. However more detailed experiments should be done to examine this in more detail, especially using cells with shRNA against SMPD1, rather that transiently transfecting WT and L225P mutant SMPD1. Furthermore, it is of great interest to examine in more depth the role of ROS and to test the top hits of the mass spectrometry data. The next step, in continuing this project would be to validate the possible novel interactions of these proteins with SMPD1. Then using this information, do design supplementary experiments in order to elucidate the mechanism by

which SMPD1 is able to influence these key signalling pathways, involved in the host's defense against bacterial infection.

References

- 1. Toth, B., Erdos, M., Sxekely, A., Ritli, L., Bagossi, P., Sumegi, J. & L. Marodi. Molecular genetic characterization of novel sphingomyelin phosphodiesterase 1 mutations causing niemann-pick disease. *JIMD Rep* 3, 125-129 (2012).
- 2. da Veiga, PL., Desnick, RJ., Adler, DA., Disteche, CM., & EH. Schuchman. Regional assignment of the human acid sphingomyelinase gene (SMPD1) by PCR analysis of somatic cell hybrids and in situ hybridization to 11p15.1----p15.4. *Genomics* **9**, 229-234 (1991).
- 3. Chan, WC., Lai, KS., & D, Todd. Adult Neimann-Pick disease: a case report. *Journal of Pathology* **121**, 177-181 (1977).
- 4. Guillemot, N., Troadec, C., de Villemeur, TB., Clement, A. & B. Fauroux. Lung disease in Niemann-Pick disease. *Pediatric Pulmonology* **42**, 1207-1214 (2007).
- 5. Lever, A.M. & Ryder, J.B. Cor pulmonale in an adult secondary to Niemann-Pick disease. *Thorax* **38**, 873-874 (1983).
- 6. Davies, J.P., Chen, F.W. & Ioannou, Y.A. Transmembrane molecular pump activity of Niemann-Pick C1 protein. *Science* **290**, 2295-2298 (2000).
- 7. Tam, C., Idone, V., Devlin, C., Fernandes, MC., Flannery, A., He, X., Schuchman, E., Tabas, I. & NW. Andrews. Exocytosis of acid sphingomyelinase by wounded cells promotes endocytosis and plasma membrane repair. *J Cell Biol* **189**, 1027-1038 (2010).
- 8. Schuchman, E.H. The pathogenesis and treatment of acid sphingomyelinase-deficient Niemann-Pick disease. *Int J Clin Pharmacol Ther* **47 Suppl 1**, S48-57 (2009).
- 9. Schuchman, E.H. The pathogenesis and treatment of acid sphingomyelinase-deficient Niemann-Pick disease. *J Inherit Metab Dis* **30**, 654-663 (2007).
- 10. Guoqiang, H. & R. Kolesnick. *Using ASMase Knockout Mice to Model Human Diseases*, (Springer-Verlag Wien, New York, 2013).
- 11. Kolak, M., Gertow, J., Westerbacka, J., Summers, SSA., Liska, J., Franco-Cereceda, A., Oresic, M., Yki-Jarvinen, H., Erikson, P. & RM., Fisher. Expression of ceramide-metabolising enzymes in subcutaneous and intraabdominal human adipose tissue. *Lipids Health Dis* 11, 115 (2012).
- 12. Dardis, A., Zampieri, S., Filocamo, M., Burlina, A., Bembi, B. & MG. Pettis. Functional In Vitro Characterization of 14 SMPD1 Mutations Identified in Italian Patients Affected by Niemann Pick Type B Disease. *Hum Mutat* **26**, 164 (2005).
- 13. Desnick, J.P., Kim, J., He, X., Wasserstein, MP, Simonaro, CM. & EH. Schuchman. Identification and characterization of eight novel SMPD1

- mutations causing types A and B Niemann-Pick disease. *Mol Med* **16**, 316-321 (2010).
- 14. Perrotta, C., Bizzozero, L., Cazzato, D., Morlacchi, S., Assi, E., Simbari, F., Zhang, Y., Gulbins, E., Bassi, MT., Rosa, P. & E. Celmenti. Syntaxin 4 is required for acid sphingomyelinase activity and apoptotic function. *J Biol Chem* **285**, 40240-40251 (2010).
- 15. Lansmann, S. Human acid sphingomyelinase. *Eur J Biochem* **270**, 1076-1088 (2003).
- 16. Becker, K.A., Grassme, H., Zhang, Y. & Gulbins, E. Ceramide in Pseudomonas aeruginosa infections and cystic fibrosis. *Cell Physiol Biochem* **26**, 57-66 (2010).
- 17. Teichgraber, V., Ulrich, M., Endlich, N., Rethmuller, J., Wilker, B., de Oliveira- Munding, CC., van Heeckeren, AM., Barr, ML., von Kurthy, G., Schmid, KW., Weller, M., Tummler, B., Lang, F., Grassme, H., Doring, G. & E. Gulbins. Ceramide accumulation mediates inflammation, cell death and infection susceptibility in cystic fibrosis. *Nat Med* 14, 382-391 (2008).
- 18. Smith, E.L. & Schuchman, E.H. Acid sphingomyelinase overexpression enhances the antineoplastic effects of irradiation in vitro and in vivo. *Mol Ther* **16**, 1565-1571 (2008).
- 19. Henry, B., Ziobro, R., Becker, K.A., Kolesnick, R. & Gulbins, E. Acid sphingomyelinase. *Handb Exp Pharmacol*, 77-88 (2013).
- 20. Miranda SR., He, X., Simonaro, CM., Gatt, S., Dagan, A., Desnick, RJ. & EH. Schuchman. Infusion of recombinant human acid sphingomyelinase into niemann-pick disease mice leads to visceral, but not neurological, correction of the pathophysiology. *FASEB* **14**, 1988-1995 (2000).
- 21. Horinouchi, K., Erlich, S., Perl, DP., Ferlinz, K., Bisgaier, CL., Sandhoff, K., Desnick, RJ., Stewart, CL. & EH. Schuchman. Acid sphingomyelinase deficient mice: a model of types A and B Niemann-Pick disease. *Nat Genet* **10**, 288-293 (1995).
- 22. Otterbach, B. & Stoffel, W. Acid sphingomyelinase-deficient mice mimic the neurovisceral form of human lysosomal storage disease (Niemann-Pick disease). *Cell* **81**, 1053-1061 (1995).
- 23. Schenck, M., Carpinteiro, A., Grassme, H., Lang, F. & Gulbins, E. Ceramide: physiological and pathophysiological aspects. *Arch Biochem Biophys* **462**, 171-175 (2007).
- 24. Puren, A.J., Fantuzzi, G., Gu, Y., Su, M.S. & Dinarello, C.A. Interleukin-18 (IFNgamma-inducing factor) induces IL-8 and IL-1beta via TNFalpha production from non-CD14+ human blood mononuclear cells. *J Clin Invest* **101**, 711-721 (1998).
- 25. Inoue, H., Massion, PP., Ueki, IF., Grattan, KM., Hara, M., Dohrman, AF., Chan, B., Lausier, JA., Golden, JA. & JA. Nadel. Pseudomonas stimulates interleukin-8 mRNA expression selectively in airway epithelium, in gland ducts, and in recruited neutrophils. *Am J Respir Cell Mol Biol* 11, 651-663 (1994).

- 26. Buccoliero, R., Ginzburg, L. & Futerman, A.H. Elevation of lung surfactant phosphatidylcholine in mouse models of Sandhoff and of Niemann-Pick A disease. *Journal of Inherited Metabolic Disease* 27, 641-648 (2004).
- 27. Scotet, V., de Braekeleer, M., Roussey, M., Rault, G., Parent, P., Dagorne, M., Journel, H., Lemoigne, A., Codet, JP., Catheline, M., David, V., Chaventré, A., Duguépéroux, I., Verlingue, C., Quéré, I., Mercier, B., Audrézet, MP., & Férec C. Neonatal screening for cystic fibrosis in Brittany, France: assessment of 10 years' experience and impact on prenatal diagnosis. *Lancet* 356, 789-794 (2000).
- 28. Knowles, M., Gatzy, J. & Boucher, R. Increased bioelectric potential difference across respiratory epithelia in cystic fibrosis. *N Engl J Med* **305**, 1489-1495 (1981).
- 29. Riordan, J.R., Rommens, JM., Kerem, B., Alon, N., Rozmahael, R., Grzelczak, Z., Zielenski, J., Lok, S., Plavsic, N., Chou, JL., *et al.*. Identification of the cystic fibrosis gene: cloning and characterization of complementary DNA. *Science* **245**, 1066-1073 (1989).
- 30. Kerem, B.S., Rommens, HM., Buchanan, JA., Markiewicz, D., Cox, TK., Chakravarti, A., Buchwald, M. & LC. Tsui. Identification of the cystic fibrosis gene: genetic analysis. *Science* **245**, 1073-1080 (1989).
- 31. Puchelle, E., Bajolet, O. & Abely, M. Airway mucus in cystic fibrosis. *Paediatric Respiratory Reviews* **3**, 115-119 (2002).
- 32. Matsui, H., Davis, C.W., Tarran, R. & Boucher, R.C. Osmotic water permeabilities of cultured, well-differentiated normal and cystic fibrosis airway epithelia. *J Clin Invest* **105**, 1419-1427 (2000).
- 33. Schwiebert, L.M., Estell, K. & Propst, S.M. Chemokine expression in CF epithelia: implications for the role of CFTR in RANTES expression. *Am J Physiol* **276**, C700-710 (1999).
- 34. Buzzetti, R., Salvatore, D., Baldo, E., Forneris, MP., Lucidi, W., Manunza, D., Marinelli, I., Messore, B., Neri, AS., Raia, V., Furnari, ML. & G. Mastella.. An overview of international literature from cystic fibrosis registries: 1. Mortality and survival studies in cystic fibrosis. *J Cyst Fibros* 8, 229-237 (2009).
- Zhao, J., Zhao, J., Schloss, PD., Kalikin, LM., Carmody, LA., Foster, BK., Petrosino, JF., Cavalcoli, JD., van Devanter, DR., Murray, S., li, JZ., Young, VB. & JJ. Li Puma. Decade-long bacterial community dynamics in cystic fibrosis airways. *Proc Natl Acad Sci U S A* 109, 5809-5814 (2012).
- Davies, J.C. Pseudomonas aeruginosa in cystic fibrosis: pathogenesis and persistence. *Paediatr Respir Rev* **3**, 128-134 (2002).
- 37. McGuigan, L. & Callaghan, M. The evolving dynamics of the microbial community in the cystic fibrosis lung. *Environ Microbiol* (2014).
- 38. Ehre, C., Ridley, C. & Thornton, D.J. Cystic fibrosis: An inherited disease affecting mucin-producing organs. *Int J Biochem Cell Biol* **52**, 136-145 (2014).

- 39. Becker, K.A., Riethmuller, J., Luth, A., Doring, G., Kleuser, B. & E. Gulbins. Acid sphingomyelinase inhibitors normalize pulmonary ceramide and inflammation in cystic fibrosis. *Am J Respir Cell Mol Biol* **42**, 716-724 (2010).
- 40. Becker, K.A., Riethmuller, J., Zhang, Y. & Gulbins, E. The role of sphingolipids and ceramide in pulmonary inflammation in cystic fibrosis. *Open Respir Med J* **4**, 39-47 (2010).
- 41. Ulrich, M., Worlitzsch, D., Viglio, S., Siegmann, N., Iadarola, P., Shute, JK., Geiser, M., Pier, GB., Friedel, G., Barr, ML., Schuster, A., Meyer, KC., Ratjen, F., Bjarnsholt, T., Gulbins, E. & G. Doring. Alveolar inflammation in cystic fibrosis. *J Cyst Fibros* 9, 217-227 (2010).
- 42. Ziobro, R., Henry, B., Edwards, M.J., Lentsch, A.B. & Gulbins, E. Ceramide mediates lung fibrosis in cystic fibrosis. *Biochem Biophys Res Commun* **434**, 705-709 (2013).
- 43. Riethmuller, J., Anthonysamy, J., Serra, E., Schwab, M., Doring, G. & E. Gulbins. Therapeutic efficacy and safety of amitriptyline in patients with cystic fibrosis. *Cell Physiol Biochem* **24**, 65-72 (2009).
- 44. http://www.webmd.com/drugs/2/drug-8611/amitriptyline-oral/details. in *WebMD*, Vol. 2014 (2014).
- 45. Houman Ashrafian, John D. Horowitz & Frenneaux, M.P. Perhexiline. *Cardiovascular Therapuetics* **25**, 76-97 (2007).
- 46. Cuenda, A. & Rousseau, S. p38 MAP-Kinases pathway regulation, function and role in human diseases. *Biochim Biophys Acta* **1773**, 1358-1375 (2007).
- 47. Bohm, M., Schroder, H.C., Muller, I.M., Muller, W.E.G. & Gamulin, V. The mitogen-activated protein kinase p38 pathway is conserved in metazoans: cloning and activation of p38 of the SAPK2 subfamily from the sponge Suberites domuncula. *Biology of the Cell* **92**, 95-104 (2000).
- 48. Li, M., Liu, J. & Zhang, C. Evolutionary history of the vertebrate mitogen activated protein kinases family. *PLoS One* **6**, e26999 (2011).
- 49. Liu, Y., Shepherd, E.G. & Nelin, L.D. MAPK phosphatases--regulating the immune response. *Nat Rev Immunol* 7, 202-212 (2007).
- 50. Ono, K. & Han, J. The p38 signal transduction pathway: activation and function. *Cell Signal* **12**, 1-13 (2000).
- 51. Chen, Z., Beers Gibson, T., Robinson, F., Silvestro, L., Pearson, G., Xu, B., Wright, A., Vanderbilt, C. & M. Cobb. MAP Kinases. *American Chemical Society* **101**, 2449-2476 (2001).
- 52. Roux, P.P. & Blenis, J. ERK and p38 MAPK-activated protein kinases: a family of protein kinases with diverse biological functions. *Microbiology and Molecular Biology Reviews* **68**, 320-+ (2004).
- 53. Zhang, Y.L. & Dong, C. MAP kinases in immune responses. *Cell Mol Immunol* **2**, 20-27 (2005).
- 54. Shirakabe, K., Yamaguchi, K., Shibuya, H., Irie, K., Matsuda, S., Moriguchi, T., Gotoh, Y., Matsumoto, K. & E. Nishida. TAK1 mediates the ceramide signaling to stress-activated protein kinase/c-Jun N-terminal kinase. *J Biol Chem* **272**, 8141-8144 (1997).

- 55. Irie, T., Muta, T. & Takeshige, K. TAK1 mediates an activation signal from toll-like receptor(s) to nuclear factor-kappaB in lipopolysaccharide-stimulated macrophages. *FEBS Lett* **467**, 160-164 (2000).
- 56. Lee, J., Mira-Arbibe, L. & Ulevitch, R.J. TAK1 regulates multiple protein kinase cascades activated by bacterial lipopolysaccharide. *J Leukoc Biol* **68**, 909-915 (2000).
- 57. Arthur, J.S. & Ley, S.C. Mitogen-activated protein kinases in innate immunity. *Nat Rev Immunol* **13**, 679-692 (2013).
- 58. Thompson, A.B., Robbins, RA., Romberger, DJ, Sisson, JH., Spurzem, JR., Teschler, H. & SI. Rennard. Immunological functions of the pulmonary epithelium. *Eur Respir J* **8**, 127-149 (1995).
- 59. Hirota, J.A. & Knight, D.A. Human airway epithelial cell innate immunity: relevance to asthma. *Curr Opin Immunol* **24**, 740-746 (2012).
- 60. Ronald G. Crystal, Scott H. Randell, John F. Engelhardt, Judith Voynow & Sunday, M.E. Airway Epithelial Cells. *Proceedings of the American Thoracic Society* **5**, 772-777 (2008).
- 61. Holtzman, M.J., Byers, D.E., Alexander-Brett, J. & Wang, X. The role of airway epithelial cells and innate immune cells in chronic respiratory disease. *Nat Rev Immunol* **14**, 686-698 (2014).
- 62. Ganesan, S., Comstock, A.T. & Sajjan, U.S. Barrier function of airway tract epithelium. *Tissue Barriers* 1, e24997 (2013).
- 63. Lampinen, M., Carlson, M., Hakansson, L.D. & Venge, P. Cytokine-regulated accumulation of eosinophils in inflammatory disease. *Allergy* **59**, 793-805 (2004).
- 64. Nicholas A. Eisele & Anderson, D.M. Host Defense and the Airway Epithelium: Frontline Responses That Protect against Bacterial Invasion and Pneumonia. *Journal of Pathogens* **2011**(2011).
- 65. Anders, H.J., Banas, B. & Schlondorff, D. Signaling danger: Toll-like receptors and their potential roles in kidney disease. *Journal of the American Society of Nephrology* **15**, 854-867 (2004).
- 66. Kawai, T. & Akira, S. The role of pattern-recognition receptors in innate immunity: update on Toll-like receptors. *Nat Immunol* **11**, 373-384 (2010).
- 67. Raoust, E., Balloy, V., Garcia-Verugo, I., Touqui, L., Ramophai, R., & M. Chignard. Pseudomonas aeruginosa LPS or flagellin are sufficient to activate TLR-dependent signaling in murine alveolar macrophages and airway epithelial cells. *PLoS One* 4, e7259 (2009).
- 68. Buchholz, B.M. & Bauer, A.J. Membrane TLR Signaling Mechanisms in the Gastrointestinal Tract during Sepsis. *Neurogastroenterol Motil* **22**, 232-245 (2010).
- 69. Beaudoin, T., LaFayette, S., Roussel, L., Berube, J., Desrosiers, M., Nguyen, D. & S. Rousseau. The level of p38alpha mitogen-activated protein kinase activation in airway epithelial cells determines the onset of innate immune responses to planktonic and biofilm Pseudomonas aeruginosa. *J Infect Dis* **207**, 1544-1555 (2013).
- 70. O'Neill, L.A.J. How Toll-like receptors signal: what we know and what we don't know. *Current Opinion in Immunology* **18**, 3-9 (2006).

- 71. Baeuerle, P.A. & Henkel, T. Function and activation of NF-kappa B in the immune system. *Annu Rev Immunol* **12**, 141-179 (1994).
- 72. Singh, H., Sen, R., Baltimore, D. & Sharp, P.A. A Nuclear Factor That Binds to a Conserved Sequence Motif in Transcriptional Control Elements of Immunoglobulin Genes. *Nature* **319**, 154-158 (1986).
- 73. Oeckinghaus, A. & Ghosh, S. The NF-kappaB family of transcription factors and its regulation. *Cold Spring Harb Perspect Biol* **1**, a000034 (2009).
- 74. Baldwin, A.S., Jr. The NF-kappa B and I kappa B proteins: new discoveries and insights. *Annu Rev Immunol* **14**, 649-683 (1996).
- 75. Zandi, E., Rothwarf, D.M., Delhase, M., Hayakawa, M. & Karin, M. The IkappaB kinase complex (IKK) contains two kinase subunits, IKKalpha and IKKbeta, necessary for IkappaB phosphorylation and NF-kappaB activation. *Cell* **91**, 243-252 (1997).
- 76. Bours, V., Burd, PR., Brown, K., Villalobos, J., Park, S., Ryseck, RP., Bravo, R., Kelly, K. & U. Siebenlist. A Novel Mitogen-Inducible Gene-Product Related to P50/P105-Nf-Kappa-B Participates in Transactivation through a Kappa-B Site. *Molecular and Cellular Biology* **12**, 685-695 (1992).
- 77. Tabary O., Escotte, S., Couetil, JP., Hubert, D., Dusser, D., Puchelle, E. & Jacquot, J. Relationship between IkappaBalpha deficiency, NFkappaB activity and interleukin-8 production in CF human airway epithelial cells. *European Journal of Physiology* 443 (2001).
- 78. El-Hashim, A.Z., Renno, WM., Abduo, HT., Jaffal, SM., Akhtar, S. & IF. Benter. Effect of inhibition of the ubiquitin-proteasome-system and IkappaB kinase on airway inflammation and hyperresponsiveness in a murine model of asthma. *Int J Immunopathol Pharmacol* **24**, 33-42 (2011).
- 79. Kuno K, Sukegawa K, Ishikawa Y, Orii T & K., M. Acid sphingomyelinase is not essential for the IL-1 and tumor necrosis factor receptor signaling pathway leading to NFkB activation. *International Immunology* **6**, 1269-1272 (1994).
- 80. Zhang, Y., Li, X., Becker, K.A. & Gulbins, E. Ceramide-enriched membrane domains--structure and function. *Biochim Biophys Acta* **1788**, 178-183 (2009).
- 81. Petrache, I,. Kamocki, K., Poirier, C., Pewzner-Jung, Y., Laviad, EL., Schweitzer, KS., van Denmark, M., Justice, MJ., Hubbard, WC. & AH. Futerman. Ceramide synthases expression and role of ceramide synthase-2 in the lung: insight from human lung cells and mouse models. *PLoS One* **8**, e62968 (2013).
- 82. Zeidan, Y.H. & Hannun, Y.A. Activation of Acid Sphingomyelinase by Protein Kinase C δ-mediated Phosphorylation. *The Journal of Biological Chemistry* **282**, 11549-11561 (2007).
- 83. Grassme, H., Jendrossek, V., Riehle, A., von Kurthy, G., Berger, J., Schwarz, H., Weller, M., Kolesnick, R. & E. Gulbins. Host defense

- against Pseudomonas aeruginosa requires ceramide-rich membrane rafts. *Nat Med* **9**, 322-330 (2003).
- 84. Chen, CL., Lin, CF., Chang, WT., Huang, WC., Teng, CF. & YS.Lin. Ceramide induces p38 MAPK and JNK activation through a mechanism involving a thioredoxin-interacting protein-mediated pathway. *Blood* 111, 4365-4374 (2008).
- 85. Wojewodka, G., De Sanctis, J.B. & Radzioch, D. Ceramide in cystic fibrosis: a potential new target for therapeutic intervention. *J Lipids* **2011**, 674968 (2011).
- 86. Grassme, H., Jekle, A., Riehle, A., Schwarz, H., Berger, J., Sandhoff, K., Kolesnick, R. & E. Gulbins. CD95 signaling via ceramide-rich membrane rafts. *J Biol Chem* **276**, 20589-20596 (2001).
- 87. Savić, R. & Schuchman, E.H. Use of Acid Sphingomyelinase for Cancer Therapy. *Advances in Cancer Research* **117**, 91-115 (2013).
- 88. Berube, J., Roussel, L., Nattagh, L. & Rousseau, S. Loss of Cystic Fibrosis Transmembrane Conductance Regulator Function Enhances Activation of p38 and ERK MAPKs, Increasing Interleukin-6 Synthesis in Airway Epithelial Cells Exposed to Pseudomonas aeruginosa. *J Biol Chem* **285**, 22299-22307 (2010).
- 89. Lee, J.C., Laydon, JT., McDonnell, PC., Gallagher, TF., Kumar, S., Green, D., McNulty, D., Blumenthal, MJ., Heys, JR., Landvatter, SW., *et al.* A protein kinase involved in the regulation of inflammatory cytokine biosynthesis. *Nature* **372**, 739-746 (1994).
- 90. Shapiro, L. & Dinarello, C.A. Osmotic regulation of cytokine synthesis in vitro. *Proc Natl Acad Sci U S A* **92**, 12230-12234 (1995).
- 91. Loitsch, SM., von Mallinckrodt, C., Kippenberger, S., Steinhilber, D., Wagner, TO. & J. Bargon. Reactive oxygen intermediates are involved in IL-8 production induced by hyperosmotic stress in human bronchial epithelial cells. *Biochem Biophys Res Commun* **276**, 571-578 (2000).
- 92. Zhang, Y., Li, X., Carpinteiro, A. & Gulbins, E. Acid sphingomyelinase amplifies redox signaling in Pseudomonas aeruginosa-induced macrophage apoptosis. *J Immunol* **181**, 4247-4254 (2008).
- 93. Manthey, C. & Schuchman, E.H. Acid sphingomyelinase-derived ceramide is not required for inflammatory cytokine signalling in murine macrophages. *Cytokine* **9**(1998).
- 94. Bauer, J., Huy, C., Brenmoehl, J., Obermeier, F. & Bock, J. Matrix metalloproteinase-1 expression induced by IL-1beta requires acid sphingomyelinase. *FEBS Lett* **583**, 915-920 (2009).
- 95. Perry, D.M., Newcomb, B., Adada, M., Wu, BX., Roddy, P., Kitatani, K., Siskind, L., Obeid, LM. & YA. Hannun. Defining a role for acid sphingomyelinase in the p38/interleukin-6 pathway. *J Biol Chem* **289**, 22401-22412 (2014).
- 96. Matsuzawa, A., Saegusa, K., Noguchi, T., Sadamitsu, C., Nishitoh, H., Nagai, S., Koyasu, S., Matsumoto, K., Takeda, K. & I. Ichijo.. ROSdependent activation of the TRAF6-ASK1-p38 pathway is selectively

- required for TLR4-mediated innate immunity. *Nature Immunology* **6**, 587-592 (2005).
- 97. Dobrowsky, R.T., Kamibayashi, C., Mumby, M.C. & Hannun, Y.A. Ceramide activates heterotrimeric protein phosphatase 2A. *J Biol Chem* **268**, 15523-15530 (1993).
- 98. Cornell, T.T., Hinkovska-Galcheva, V., Sun, L., Cai, Q., Hershenson, MB., Vanway, S. & Tp. Shanley. Ceramide-dependent PP2A regulation of TNFalpha-induced IL-8 production in respiratory epithelial cells. *Am J Physiol Lung Cell Mol Physiol* **296**, L849-856 (2009).
- 99. Sakata, A., Ochiai, T., Shimeno, H., Hikishima, S., Yokomatsu, T., Shibuya, S., Toda, A., Eyanagi, R. & S. Soeda. Acid sphingomyelinase inhibition suppresses lipopolysaccharide-mediated release of inflammatory cytokines from macrophages and protects against disease pathology in dextran sulphate sodium-induced colitis in mice. *Immunology* 122, 54-64 (2007).
- 100. Irun, P., Mallen, M., Dominguez, C., Rodriguez-Sureda, V., Alvaraez-Sala, LA., Arslan, N., Bermejo, N., Guerrero, C., Perez de Soto, I., Villaln, L., Giraldo, P. & M. Pocovi. Identification of seven novel SMPD1 mutations causing Niemann-Pick disease types A and B. *Clin Genet* 84, 356-361 (2013).
- 101. Clontech. KnockoutTM Inducible RNAi Systems User Manual.
- 102. Waypa, G.B., Guzy, R., Mungai, PT., Mack, MM., Marks, JD., Roe, MW. & PT. Schumacker. Increases in mitochondrial reactive oxygen species trigger hypoxia-induced calcium responses in pulmonary artery smooth muscle cells. *Circ Res* 99, 970-978 (2006).
- 103. Gregan, J., Riedel, CG., Petronczki, M., Cipak, L., Rumpf, C., Poser, L., Bucholz, F., Mechtler, K., & K. Nasmyth. Tandem affinity purification of functional TAP-tagged proteins from human cells. *Nat Protoc* **2**, 1145-1151 (2007).
- 104. Zhang, Z., Reenstra, W., Weiner, D., Louboutin, J.P. & Wilson, J. The p38 Mitogen-Activated Protein Kinase Signaling Pathway Is Coupled to Toll-Like Receptor 5 To Mediate Gene Regulation in Response to Pseudomonas aeruginosa Infection in Human Airway Epithelial Cells. *Infection and Immunity* 75, 5985-5992 (2007).
- 105. Martel, G., Berube, J. & Rousseau, S. The Protein Kinase TPL2 Is Essential for ERK1/ERK2 Activation and Cytokine Gene Expression in Airway Epithelial Cells Exposed to Pathogen-Associated Molecular Patterns (PAMPs). *PLOSone* **8**(2013).
- 106. Roussel, L., Martel, G., Berube, J. & Rousseau, S. P. aeruginosa drives CXCL8 synthesis via redundant toll-like receptors and NADPH oxidase in CFTRF508 airway epithelial cells. *J Cyst Fibros* **10**, 107-113 (2011).
- 107. Conese, M., Copreni, E., Di Gioia, S., De Rinaldis, P. & Fumarulo, R. Neutrophil recruitment and airway epithelial cell involvement in chronic cystic fibrosis lung disease. *J Cyst Fibros* **2**, 129-135 (2003).
- 108. Denes, A., Lopex-Castejon, G. & Brough, D. Caspase-1: is IL-1 just the tip of the ICEberg? *Cell Death and Disease* **3**(2012).

- 109. Puren, A.J., Fantuzzi, G. & Dinarello, C.A. Gene expression, synthesis, and secretion of interleukin 18 and interleukin 1beta are differentially regulated in human blood mononuclear cells and mouse spleen cells. *Proc Natl Acad Sci U S A* **96**, 2256-2261 (1999).
- 110. Satelli, A. & Li, S. Vimentin as a potential molecular target in cancer therapy Or Vimentin, an overview and its potential as a molecular target for cancer therapy. *Cell Mol Life Science* **68**, 3033-3046 (2012).
- 111. Katsumoto, T., Mitsushima, A. & Kurimura, T. The role of the vimentin intermediate filaments in rat 3Y1 cells elucidated by immunoelectron microscopy and computer-graphic reconstruction. *Biol Cell* **68**, 139-146 (1990).
- 112. Jang., C.-Y., Kim., H.D., Zhang., X., Chang., J.-S. & Kim., J. Ribosomal protein S3 localizes on the mitotic spindle and functions as a microtubule associated protein in mitosis. *Biochemical and Biophysical research Communications* **492**, 57-62 (2012).
- 113. Kim, Y., Kim, H.D. & Kim, J. Cytoplasmic ribosomal protein S3 (rpS3) plays a pivotal role in mitochondrial DNA damage surveillance. *Biochim Biophys Acta* **1833**, 2943-2952 (2013).
- 114. Gao, X. & Hardwidge, P.R. Ribosomal protein s3: a multifunctional target of attaching/effacing bacterial pathogens. *Front Microbiol* **2**, 137 (2011).
- 115. Tamsyn Stanborough, Johannes Niederhauser, Barbara Koch, Helmut Bergler & Pertschy, B. Ribosomal protein S3 interacts with the NF-jB inhibitor IjBa. *FEBS Letters* **588**(2014).
- 116. Wan, F., Anderson, DE., Barnitz, RA., Snow, A., Bidere, N., Zheng, L., Hegde, V., Lam, LT., Staudt, LM., Levens, D., Deutsch, WA., & MJ. Lenardo. Ribosomal Protein S3: A KH Domain Subunit in NF-kB Complexes that Mediates Selective Gene Regulation. *Cell* 131, 927-939 (2007).
- 117. Eric M. Wier, Jordan Neighoff, Xin Sun, Kai Fu & Wan, F. Identification of an N-terminal Truncation of the NF- κB p65 Subunit That Specifically Modulates Ribosomal Protein S3-dependent NF-κB Gene Expression. *The Journal of Biological Chemistry* **287**(2012).
- 118. Mahajan, K.N. & Mitchell, B.S. Role of human Pso4 in mammalian DNA repair and association with terminal deoxynucleotidyl transferase. *Proc Natl Acad Sci U S A* **100**, 10746-10751 (2003).
- Nishiyama, M., Oshikawa, K., Tsukada, Y., Nakagawa, T., Iemura, S., Natsume, T., Fan, Y., Kikuchi, A., Skoultchi, AI., & KI. Nakayama. CHD8 suppresses p53-mediated apoptosis through histone H1 recruitment during early embryogenesis. *Nature Cell Biology* 11, 172-U139 (2009).

Appendix

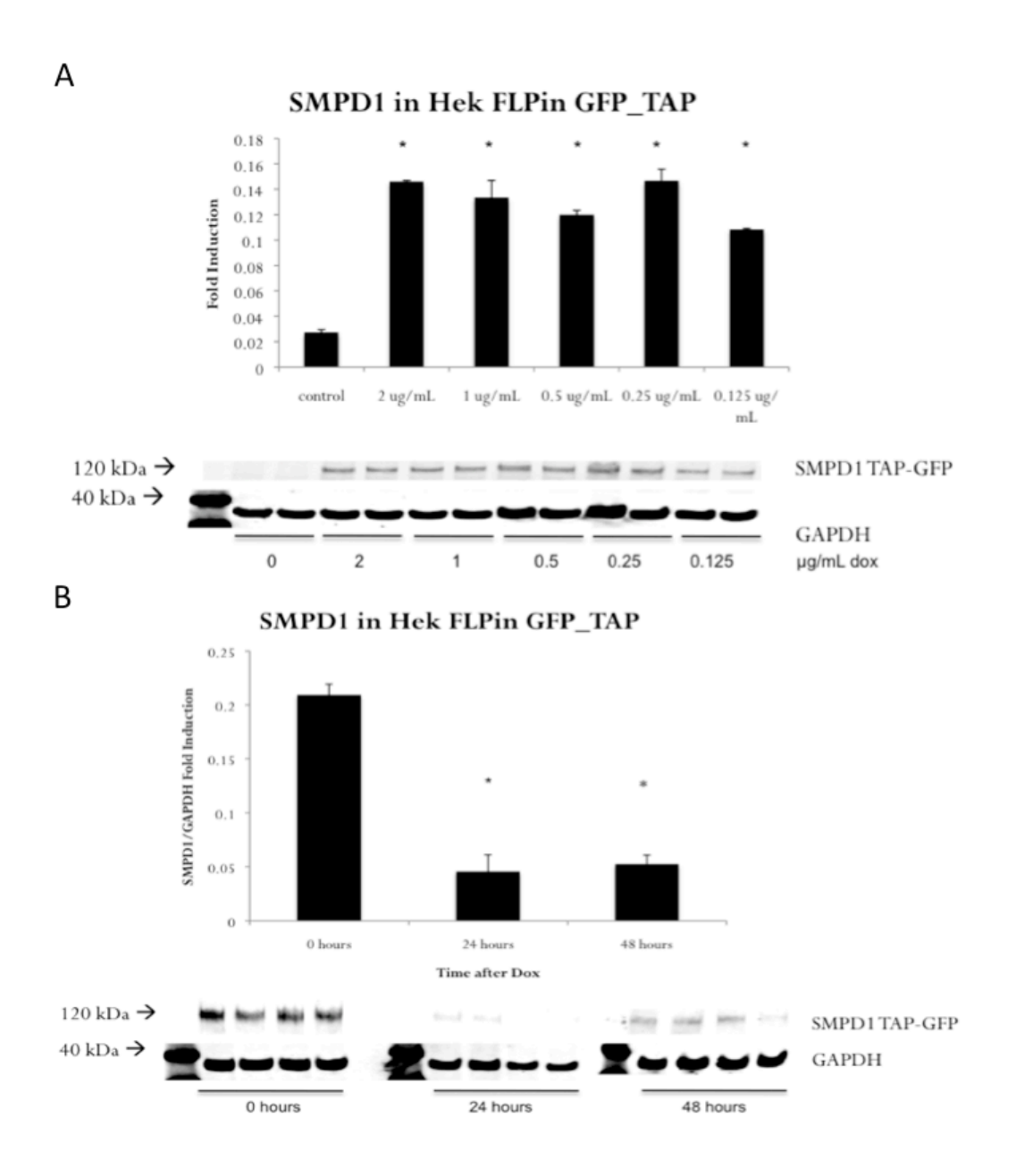


Figure 25: Creation of the Hek-Flp-IN inducible system by doxycycline.

A) Dose-dependent response for the induction of SMPD1 by doxycycline. * p<0.05 by one-way ANOVA and Dunnett's correction. B) Doxycycline chase experiment at 1 μ g/mL (repeated 3 times). * p<0.05 by one-way ANOVA and Bonferroni correction.

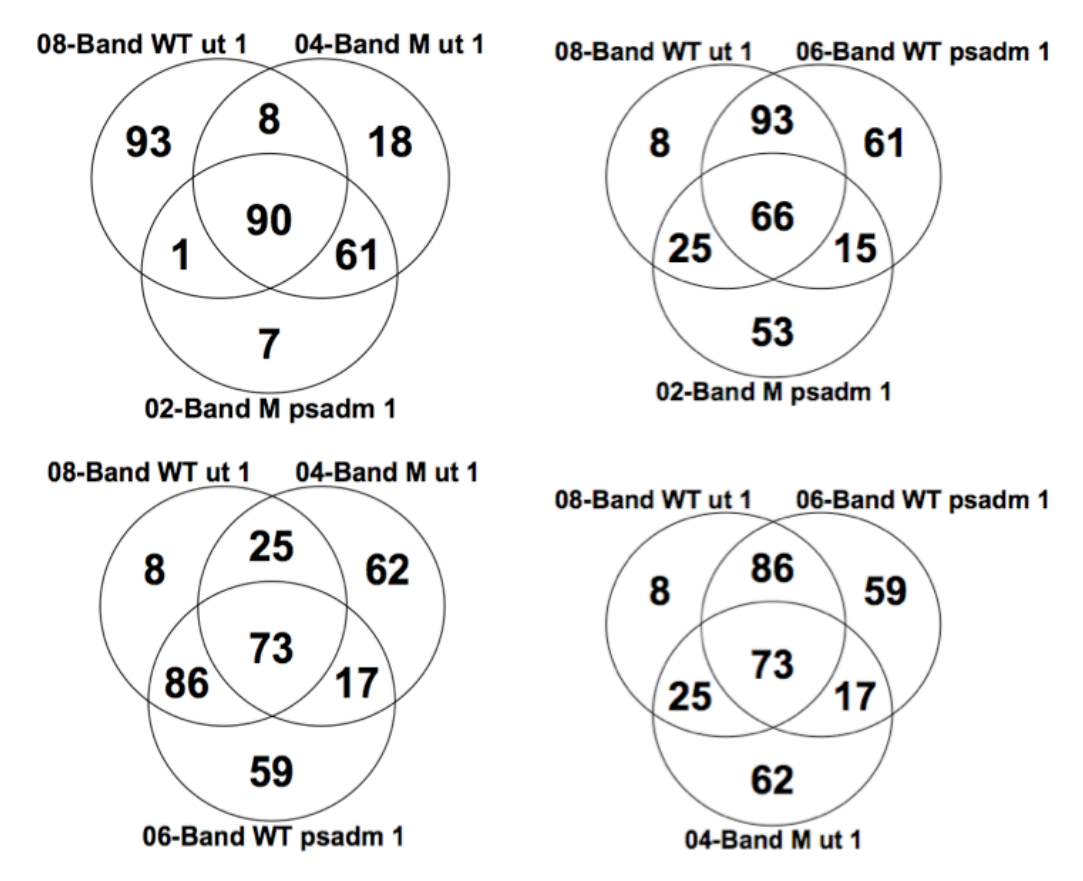


Figure 26: Venn diagrams of preliminary analysis o d mass spectrometry data using Scaffold Viewer program.

These provide preliminary analysis of the proteins identified by mass spectrometry analysis, by comparing the 4 different experimental conditions.